Integrating bio-oil and carbohydrate valorization on the fractionation of sugarcane bagasse via Organosolv process using Mo2C-based catalysts

Gleicielle Tozzi Wurzler, Victor Teixeira da Silva, Débora de Almeida Azevedo, Ayla Sant' Ana da Silva, Fabio Bellot Noronha

Integrating bio-oil and carbohydrate valorization on the fractionation of sugarcane bagasse via *Organosolv* process using Mo_2C-based catalysts

Gleicielle Tozzi Wurzler[1], Victor Teixeira da Silva[1†], Débora de Almeida Azevedo[2], Ayla Sant' Ana da Silva[3,4], Fábio Bellot Noronha[4,5]*

[1] Chemical Engineering Program, Federal University of Rio de Janeiro, Rio de Janeiro, Box 68502, 21941-914, Brazil.
[2] Chemistry Institute, Federal University of Rio de Janeiro, Rio de Janeiro, 21941-598, Brazil
[3] Biochemistry Graduation Program, Chemistry Institute Federal University of Rio de Janeiro, Rio de Janeiro, 21941-590, Brazil
[4] Catalysis, Biocatalysis and Chemical Processes Division, National Institute of Technology, Rio de Janeiro, RJ 20081-312, Brazil.
[5] Université de Lille, CNRS, Centrale Lille, Université Artois, UMR 8181 – UCCS – Unité de Catalyse et Chimie du Solide, Lille, 59000, France.
[†] *In memoriam*
*Corresponding Author: email: fabio.bellot@int.gov.br

Submitted to
Fuel Processing Technology
Revised
February 2021

Abstract

This work studied the fractionation of sugarcane bagasse via *Organosolv* treatment using isopropanol/water in the presence of Raney-Ni and molybdenum carbide catalysts (Bulk Mo_2C and Mo_2C supported on activated carbon (AC) or Al_2O_3). The degree of delignification, the bio-oil and solid residue composition depended on the type of catalyst. A partial extraction of hemicellulose occurred followed by depolymerization, resulting in a product distribution that depended on the catalyst. Raney-Ni catalyst promoted the formation of diols and triols, while xylose, furfural, and furan were mainly produced by Mo_2C based-catalysts. The *Organosolv* treatment without catalyst and in the presence of bulk Mo_2C produced a bio-oil containing mainly 2,3-dihydrobenzofuran. Mo_2C/AC and Mo_2C/Al_2O_3 are promising catalysts for the fractionation of sugarcane bagasse that produced a bio-oil with higher yield to substituted methoxyphenols and a solid residue more easily hydrolyzed by cellulases, producing higher yield to glucose than Raney-Ni catalyst.

Keywords: bio-oil; *Organosolv*; biomass fragmentation; reductive catalytic fractionation; Raney-Ni; Mo_2C

1. Introduction

Lignocellulosic biomass is a sustainable resource for the production of fuels and chemicals. However, the fractionation of lignocellulose into its major constituents (cellulose, hemicellulose and lignin) and the complete utilization of each separated fraction is still a challenge that reduces the competitiveness of the process using this feedstock. From the industrial point of view, the fractionation of lignocellulosic biomass still has issues. For instance, considering the second-generation ethanol (2G ethanol) plants that started their production in the last decade, only few of them are still under operation [1]. The delay on the technology development is partially associated with the pretreatment of biomass that was once considered a simple step of production, but it was not the reality for the large-scale operation of biorefineries [1,2]. Therefore, the search for an efficient method of fractionation of the lignocellulosic biomass is fundamental to overcome the barriers faced by a biorefinery.

Currently, large progresses have been made on the valorization of carbohydrate fractions (cellulose and hemicellulose), whereas the use of isolated lignin remains less explored, being mostly burned for energy generation [3]. However, the success of a biorefinery also requires the valorization of the lignin fraction.

Lignin, a complex and water-insoluble aromatic polymer, is derived primarily from methoxylated hydroxycinnamyl alcohol building blocks. Unlike cellulose, with a well-defined sequence of monomeric units that are linked by regular β-1,4-glycosidic bonds, lignin is characterized by a variety of distinct and chemically different bonds, each one demanding different condition for cleavage when selective depolymerization is targeted. Although structurally more complex, the higher carbon content and lower oxygen content of lignin, relative to the holocellulose fraction, renders it an attractive feedstock for the production of biofuels and chemicals [4]. In spite of the large

production of lignin by the Kraft process of the pulp and paper industry, there are no commercial process for the valorization of Kraft lignin into fuels or chemicals. This is partially due to its recalcitrant and complex chemical nature [5].

One alternative delignification technology is the so-called *Organosolv* process that uses different organic solvents/water mixtures. The solvent polarity not only affects the delignification degree, but also the fragmentation of the lignin oligomers to mono- and dimers [6]. The polarity of the solvent enhances the swelling of the lignocellulosic matrix, making it more accessible. However, the solubility of lignin oligomers (small lignin fragments with molecular weight between 100 – 400 Da) [4] significantly decreases in too polar solvents such as pure water, but water is important for the solubilization of holocellulose [7]. The combination of both counteracting effects provides a synergistic effect resulting in an increased biomass extraction and fragmentation [8].

Recently, solvents with hydrogen donor capabilities such as 2-propanol (isopropanol) have also been used on the treatment of lignocellulosic biomass [9-13] as well as on the hydrodeoxygenation of bio-oil produced [14-16]. The hydrogen donor solvents can produce *in situ* H_2 by catalytic decomposition, enhancing the solvolytic process of α-O-4 and β-O-4 ether bonds of the lignin structure and thus, promoting the fractionation of the biomass [5, 17]. The *Organosolv* process using hydrogen donor solvents has been used mostly on the fractionation of different types of wood. There are only few works about the *Organosolv* treatment of sugarcane bagasse using ethanol as solvent [12,13]. Although there are no studies about the fractionation of sugarcane bagasse using isopropanol as hydrogen donor solvent, the performance of both alcohols were similar in the fractionation of birch wood using Pd/C catalyst at 200 °C and 30 bar of H_2 for 3 h [6].

Despite the advantages of the *Organosolv* process, the repolymerization of lignin on the surface of the residual biomass can occur during the fractionation process, decreasing the efficiency of the subsequent downstream processing [18]. This is because this repolymerized lignin is characterized by very strong, highly recalcitrant C—C bonds [4]. This leads to a decrease in the efficiency of delignification, reducing the complete utilization of biomass fractions.

Recently, a new strategy for biomass fractionation has been proposed to avoid or reduce the repolymerization of lignin, the so-called reductive catalytic fractionation (RCF), in which biomass fractionation and lignin depolymerization occurs simultaneously in the presence of a heterogeneous catalyst [5,19, 20]. The role of the catalyst is to avoid repolymerization reactions by hydrogenating unsaturated lignin intermediates to monophenolic compounds. Other advantages of this catalytic fractionation process are: (i) the use of native lignin that exhibits high reactivity in comparison to isolated lignin, which is more condensed and recalcitrant; (ii) the lignin oil obtained can be upgraded under less severe conditions; (iii) the carbohydrate fraction (holocellulose) remains in the solid, whereas the lignin fraction is kept in the liquid phase, containing a high amount of aromatic compounds; and (iv) the decrease on the operational steps.

Since 2008, the number of papers about RCF has been steadily increasing but only a limited number of catalysts have been used. Most of these studies performed the fractionation in the presence of a catalyst containing noble metals such as Pd [6], Pt [21], Ru [22] or Rh [22] and transition metals such as Ni [19,20] supported on carbon or an unsupported catalyst (e.g., Raney Ni) [10,23].

Transition metal carbides are cheaper than noble metal catalysts, but exhibit similar catalytic behavior. They have been tested in a variety of reactions such as

hydrodesulfurization, hydrodenitrogenation and hydrodeoxygenation of bio-oil and model compounds representative of the lignin fraction of lignocellulose biomass [24-26] and deoxygenation of wood pyrolysis vapors [26]. Transition metal carbides have also demonstrated great potential for the conversion of lignin, exhibiting high selectivity for the cleavage of β-O-4, α-O-4, β-β and 4-O-5 bonds [25].

There are different works in the literature that reported the use of metal carbides (mainly molybdenum and tungsten) for the depolymerization of isolated lignin [27,28]. However, the catalytic fractionation of lignocellulosic biomass is much more complex, involving delignification, depolymerization and/or repolymerization of lignin fragments simultaneously. Only one work investigated the performance of metal carbide catalysts for the fractionation of lignocellulosic biomass [29]. In this work, Li *et al*. [29] reported the direct catalytic conversion of raw woody biomass into two groups of chemicals over a carbon supported Ni-W_2C catalyst. The carbohydrate fraction was converted to diols with a yield of 75.6 % (based on the amount of cellulose and hemicellulose), while the lignin component was converted selectively into monophenols with a yield of 46.5 % (based on lignin). Therefore, the metal carbide catalyst favored not only the conversion of carbohydrate fractions, but also the depolymerization of lignin, which makes it competitive when compared to noble metal catalysts.

It is also important to notice that most of the works on RCF used different types of wood (hardwoods and softwoods) [30] but only one work studied the fractionation of a grass (*Miscanthus*) using methanol and Ni/C catalyst [31]. Typical lignin structures in grasses contain ferulate, *p*-coumarate and tricin units that are not usually present in hardwoods and softwoods. Therefore, the depolymerization of lignin from grasses will produce different phenolic monomers than the ones obtained from woods.

144 Therefore, the goal of this work was to study the fractionation of sugarcane
145 bagasse (grass) via *Organosolv* treatment using isopropanol as solvent and source of
146 hydrogen (*in situ*) in the presence of different catalysts. Bulk Mo_2C and Mo_2C
147 supported on activated carbon (AC) or γ-Al_2O_3 containing 20 % (m/m) of molybdenum
148 carbide were evaluated. Raney-Ni commercial catalyst was used as reference. The
149 characterization of the bio-oil and residual biomass was carried out by GC×GC-TOFMS
150 and confocal microscopy, respectively. Both techniques provide important information
151 about the composition of the bio-oil and morphology of the residue, and they are
152 scarcely used in the literature on the biomass fractionation studies. The approach used in
153 this work allows the full transformation of the fractionated biomass into biofuels and
154 green chemicals through the integration of both lignin valorization and carbohydrate
155 upgrading. The enzymatic hydrolysis of the solid residue containing carbohydrate
156 fraction integrates the production of second-generation ethanol and the lignin extraction
157 for the bio-oil production.
158

2. Experimental

2.1. Catalyst synthesis

The bulk Mo_2C was prepared by temperature-programmed carburization (TPC) of molybdenum oxide (MoO_3, Sigma-Aldrich). The sample was heated under a 20 % CH_4/H_2 (v/v) mixture (200 mL $min^{-1}.g_{oxide}^{-1}$) at a heating rate of 2.5 °C min^{-1} from 25 to 650 °C, remaining at this temperature for 2 h. After synthesis, it was changed the gas feed to He (200 mL min^{-1}) and the system was cooled to room temperature. Since the transition metal carbides are pyrophoric, the reactor was flooded internally with isopropanol after carburization and the catalyst was removed and stored in isopropanol until its use in the reaction.

Mo_2C/AC and Mo_2C/Al_2O_3 catalysts containing 20 % (m/m) of molybdenum carbide were prepared by incipient wetness impregnation of the supports, activated carbon (AC – Merck) and ɣ-Al_2O_3 (BASF), with an aqueous solution containing ammonium heptamolybdate ($(NH_4)_6Mo_7O_{24}.4H_2O$, Merck). After impregnation, the materials were dried at 100 °C for 12 h. Then, the Mo_2C/Al_2O_3 catalyst precursor was calcined at 500 °C for 5 h. Finally, the carburization of both samples followed the procedure previously described for the bulk Mo_2C catalyst.

The nickel catalyst used was a commercial Raney-Ni 2800 slurry (Sigma-Aldrich), an active catalyst stored in water, containing Ni (≥ 89 %) and Al (6-9 %), and 20-60 µm particle size.

2.2. Catalyst Characterization

Specific surface areas of the samples were measured on a Micromeritics ASAP 2020 analyzer by N_2 adsorption at -196 °C.

Temperature-programmed carburization (TPC) experiments were performed in a homemade apparatus. The sample (100 mg) previously loaded into a quartz U-tube micro reactor was heated under a 20 % (v/v) CH_4/H_2 mixture (100 mL min^{-1}) at a heating rate of 2.5 °C min^{-1} from 25 to 650 °C, remaining at this temperature for 2 h. The gases coming out from the reactor were analyzed continuously by online mass spectrometry (Pfeiffer Vacuum QME 200) monitoring the ion signals *m/z* 16 (CH_4), *m/z* 18 (H_2O) and *m/z* 28 (CO).

Powder XRD patterns were recorded in a Bruker D8 diffractometer. The spectra were recorded in Bragg angles between 10° and 90°, with a step size of 0.02° and an acquisition time of 1 s. The crystalline phases of the samples were identified using the ICCD data base. For this characterization, the precursor oxide was *ex situ* treated by TPC and passivated at room temperature, under a mixture of 0.5 % O_2/He (30 mL min^{-1}) for 12 h.

CO chemisorption technique was carried out in order to measure the dispersion of the catalysts. The samples were activated under the same conditions previously described for the TPC experiment. Then, the samples were cooled to 30 °C and pulses of CO were injected until saturation. The dispersion was calculated assuming that one CO molecule is chemisorbed at each metal site.

2.3. Sugarcane bagasse fractionation

The delignification of sugarcane bagasse (from Iacanga plant, São Paulo - Brazil) was performed through the *Organosolv* treatment using isopropanol (iPrOH, Vetec) and water as solvents. 7 g of sugarcane bagasse and 140 mL of solvent were used. The reaction was conducted in a 300 mL autoclave (Parr reactor) at 180 °C for 3 h, under mechanical stirring at 500 rpm and autogenous pressure (Scheme 1). The

reactor was then cooled to room temperature in an ice bath. The liquor was separated from the pretreated bagasse by filtration. The pretreated bagasse retained on the filter was washed with iPrOH to remove all the compounds adsorbed thereon and then dried at 40 °C. The liquor and the washing permeate of the pretreated bagasse were mixed and placed into a rotary evaporator under vacuum at 60 °C for removal of the solvents. The bio-oil and the pretreated bagasse were kept under refrigeration for the characterization analyzes. The catalytic method was carried out similarly as *Organosolv*. 5 g of the nickel catalyst (Raney-Ni® 2800, Sigma Aldrich) was used. For the carbide catalysts, it was used 0.7 g of bulk Mo_2C, and 3.5 g of Mo_2C/AC and Mo_2C/Al_2O_3 catalysts, in order to keep the same amount of active phase.

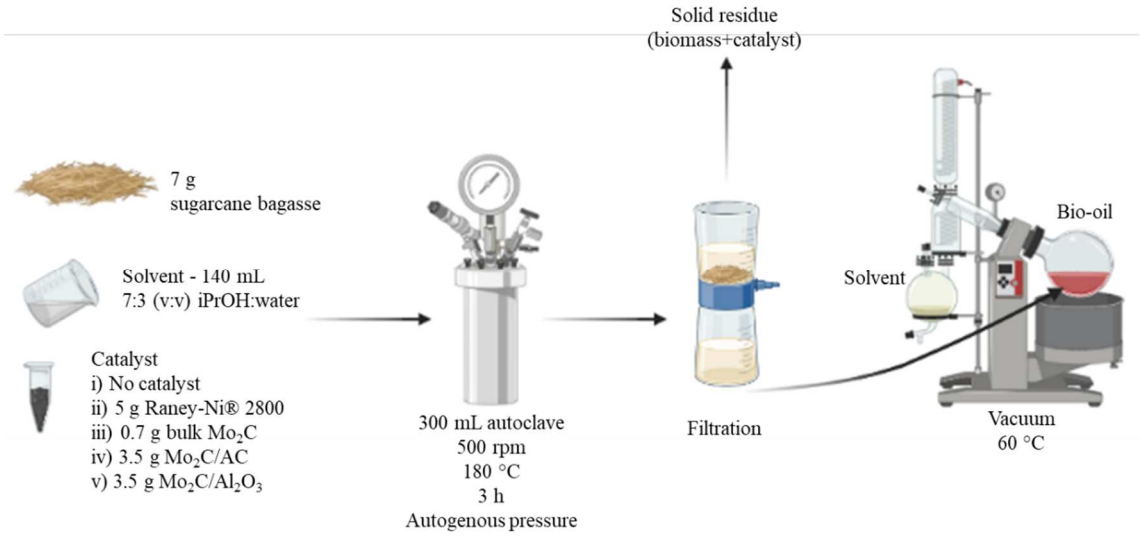

Scheme 1. Schematic diagram of experimental procedure of sugarcane bagasse fractionation.

2.4. Characterization of biomass

The chemical compositional analyses of biomass (e.g. lignin and sugars) were performed following NREL (National Renewable Energy Laboratory, USA) analytical

procedures [32]. The degree of delignification (D_{lig}) and the fraction of sugar in the pretreated bagasse (R) recovered were calculated using Eqs. 1 and 2.

$$Dlig(\%) = \frac{(f_{lignin\ total,0} - f_{lignin\ insol,f}).f_{sol.recup}}{f_{lignin\ total,0}}.100 \quad (1)$$

$$R(\%) = \frac{f_{sugarrecup} f_{sol.recup}}{f_{sugar,0}}.100 \quad \text{, where,} \quad f_{sol.recup} = \frac{m_{bagasse,f}}{m_{bagasse,0}} \quad (2)$$

where $f_{lignin\ total,0}$ is the fraction of total lignin (acid soluble and insoluble lignin) present in the bagasse before treatment and $f_{lignin\ insol,f}$ is the acid insoluble lignin fraction present in the pretreated bagasse recovered after treatment. $f_{sugar\ recup}$ is the sugar fraction in the pretreated bagasse after treatment and $f_{sugar,0}$ is the sugar fraction in the bagasse before treatment. $f_{sol.recup}$ is the fraction of solid residue recovered after the reaction (unreacted bagasse), $m_{bagasse,f}$ is the mass of unreacted bagasse, $m_{bagasse,0}$ is the mass of initial bagasse loaded into the reactor. The fraction of bio-oil formed is calculated in the same way as $f_{sol.recup}$, but considering the mass of bio-oil recovered after the rotary evaporator process.

Thermogravimetric analyzes evaluated the thermal stability of untreated and pretreated bagasse. They were run on a Hitachi STA7300, at a heating rate of 5 °C min^{-1} from room temperature to 700 °C under N_2 flow at 80 mL min^{-1}.

Confocal fluorescence imaging was carried out using a Zeiss LSM 710 confocal microscope. Untreated and pretreated bagasse samples were stained with Safranin O and Congo Red. The residues were stained with 0.1 % Safranin O for 5 min, then destained by washing in aqueous solution of 50 % ethanol at 30 °C for 3 min until the washing solution is translucent. Then, the residues were stained with 1 % Congo Red under the same conditions as Safranin O and then washed. After staining procedure, slides were

mounted with Fluoromount-G®. Sections stained were excited at 488 nm wavelength. The confocal microscopy images of cellulose and lignin were collected in the 497-544 nm and 561-603 nm spectral regions, respectively. Samples were observed using an LD Plan-Neofluar 40x/0.6 Korr M27 and LD Plan-Neofluar 20x/0.6 Korr M27 objective, and each 1 mm thick image series was rendered as a maximum projection (2D) image from the Z-stack) with an image size of 1024 × 1024 pixels. Images were treated using Image J software v. 1.52e.

2.5. Characterization of bio-oil

Thermogravimetric analyzes of bio-oils were performed on a Hitachi STA7300, using the same conditions previously described for the biomass. TGA experiments of the liquid product, performed under an inert atmosphere, were used for estimating the fraction of volatile compounds at the injector temperature of the chromatograph [10].

In order to analyze the bio-oils via GC×GC-TOFMS, approximately 13.0 mg of each bio-oil sample were weighed using an analytical balance and dissolved with 2.0 mL of methanol solvent. Then, the solutions were filtered in 0.2 μm syringe filters and dried in a N_2 stream. The samples were resolubilized with 0.5 mL of the standard mixture followed by the chromatographic analysis. Standard mixture was composed of deuterated internal standards, used for identification and semi-quantification, were obtained from CDN Isotopes (Quebec, Canada) and have purity greater than 97 %: toluene-D_8, 1-heptanol-D_{15}, hexanoic acid-D_{11}, phenol-D_6, decalin-D_{18}, hexadecane-D_{34} and 5α-cholestane-D_6.

The GC×GC-TOFMS system used was a Pegasus 4D (Leco, St. Joseph, MI, USA), which includes an Agilent Technologies 7890 GC (Palo Alto, CA, USA) equipped with a secondary oven, a non- moving quad-jet dual-stage modulator, and a

Pegasus H11 (Leco, St. Joseph, MI, USA) time-of-flight mass spectrometer. The GC columns consisted of a DB-5 (Agilent Technologies, Palo Alto, CA, USA) with 5 %-phenyl –95 %-methylsiloxane (30 m × 0.25 mm i.d., 0.25 μm df) as the first dimension column (^{1}D) and a DB-17 (Agilent Technologies, Palo Alto, CA, USA) with 50 %-phenyl–50 %-methylsiloxane (1.2 m × 0.1 mm i.d., 0.1 μm df) as the second dimension column (^{2}D). The ^{2}D column was connected to the TOFMS via a 0.5 m × 0.25 mm i.d. empty deactivated fused silica capillary using SGE mini-unions and SilTite™ metal ferrules 0.1–0.25 mm i.d. (Ringwood, VIC, Australia). The injections were performed in a splitless mode of 1 μL at 300 °C using a purge time of 60 s and a purge flow of 5 mL min^{-1}. Helium (99.9999 % purity) was used as carrier gas at a constant flow rate of 1.0 mL min^{-1}. The chromatographic conditions were optimized. The primary oven temperature program was 40 °C for 5 min and ramped up to 320 °C at 5 °C min^{-1}. The temperature of the secondary oven was 5 °C higher than that of the primary oven. Modulation period was 5 s, with a 1.5 s hot-pulse and 1.0 s cool-pulse duration, with modulator temperature 30 °C higher than the primary oven temperature. The MS transfer line was maintained at 300 °C, and the TOFMS was operated in the electron ionization mode with a collected mass range of *m/z* 35–600. The ion source temperature was 230 °C, the detector was operated at −1400 V, with electron energy 70 eV, and an acquisition rate of 100 spectra s^{-1}.

GC×GC-TOFMS data acquisition and processing were performed using ChromaTOF® software version 4.5 (Leco, St. Joseph, MI, USA). Samples were submitted to a data-processing method for which the individual peaks were automatically detected based on a 500:1 signal-to-noise ratio. The areas of individual peaks were acquired using the base peak of each spectrum, generating a list of all detected peaks. The relative area was calculated by peak area/total area of compounds

300 detected with signal-to-noise ratio higher than 500:1, excluding the solvent area.
301 Identification was performed by comparing the deconvoluted mass spectrum obtained
302 with the NIST Mass Spectral Library software (NIST 08, Software Version: 2.0) for
303 correct matching, in addition to the retention times and elution order of the authentic
304 standards. After comparison, only peaks with similarities greater than 80 % were
305 identified.
306
307 ***2.6. Enzymatic hydrolysis of untreated and pretreated bagasse samples***
308 Enzymatic hydrolysis of untreated and pretreated bagasses samples were carried
309 out with the commercial enzymes Celluclast 1.5L and Novozyme 188. The activity of
310 the enzymes was measured as previously described in the literature [33]. A unit of β-
311 glucosidase (BGU) was defined as the amount of enzyme that converted 1 μmol of
312 cellobiose to glucose in 1 min and a unit of FPase (FPU) corresponds to the release of 1
313 μmol of glucose per minute at 50 °C.
314 Enzymatic hydrolysis was performed in duplicate assays using 0.5 g biomass
315 (dry weight) in 50 mL glass vials flasks containing sodium citrate buffer (0.05 M), at
316 pH 4.8 and enzymes, in an assay of 10 g (total mass), reaching solids content of 5 %
317 (m/m). In these assays, a mixture of commercial enzymes Celluclast 1.5L and
318 Novozyme 188 at FPU:BGU ratio of 1:3 was used as sources of cellulases and beta-
319 glucosidase, respectively. The cellulase (Celluclast) dosage for enzymatic hydrolysis
320 was 20 FPU g^{-1} of glucans. Sodium azide (0.01 g) was added to prevent the growth of
321 microorganisms.
322 The flasks were sealed and kept in a rotary incubator maintained at 50 °C and
323 200 rpm. Samples were collected at 2, 4, 6, 24, 48 and 72 h, and only 10 % of the initial
324 total volume was withdrawn. Each aliquot was transferred to tubes which were kept in a

boiling water bath for 5 min in order to denature the enzyme pool. Subsequently they were centrifuged and the supernatants were submitted for glucose quantification in the biochemical analyzer (YSI 2700 Select TM, Marshall Scientific).

The glucose yield was calculated according to Eq. 3.

$$Y_{glucose} = \frac{(C_{glucose} - C_{glucose,0})}{1.111\left(w_t / V_{h0}\right) F_{ins,0} \cdot F_{glucan}} \cdot 100 \quad (3)$$

where $C_{glucose}$ is the concentration of glucose in the hydrolysate (g L^{-1}), $C_{glucose,0}$ is the initial glucose concentration in the hydrolysis assay, w_t is the total mass of the hydrolysis assay (g), V_{h0} is the initial volume of liquid (L), *wt* corresponds to the initial mass of liquid added to the hydrolysis assay, $F_{ins,0}$ is the initial mass fraction insoluble in the total hydrolysis assay, F_{glucan} is the initial mass fraction of glucans in the solid insoluble.

3. Results and discussion

3.1. Catalyst Characterization

The BET surface areas of the catalysts increased from 25 m^2 g^{-1} for the bulk Mo_2C to 540 m^2 g^{-1} and 165 m^2 g^{-1} for Mo_2C/AC and Mo_2C/Al_2O_3, respectively.

Fig. 1 shows the profiles of different products formed during treatment under 20 % CH_4/H_2 (v/v) mixture: *m/z* 18 (H_2O); *m/z* 28 (CO) and *m/z* 16 (CH_4). For the bulk Mo_2C, the curve corresponding to water shows a shoulder at 625 °C and a peak at 640 °C. However, there is only one peak at 650 °C on the curves of the *m/z* 28 and 16 signals. This result indicates that the first peak in the curve of *m/z* 18 corresponds to the reduction of MoO_3 to MoO_2 with water formation (Eq. 4). The second peak in the *m/z* 18 curve is followed by the consumption of methane and the formation of CO, suggesting the formation of Mo carbide (Eq. 5). The same results are reported in the literature [34].

$$MoO_3 + H_2 \rightarrow MoO_2 + H_2O \quad (4)$$

$$2MoO_2 + 2CH_4 \rightarrow Mo_2C + 3H_2O + CO + H_2 \quad (5)$$

For the supported samples, the profiles corresponding to water are more complex than that one for bulk sample. Mo_2C/AC exhibited peaks at 361 and 550 °C while three peaks are observed on the profile of Mo_2C/Al_2O_3 catalyst at 357, 403 and 560 °C. It is observed the formation of CO above 500 °C, with a peak at around 650 °C, which is followed by a peak with weak intensity corresponding to the consumption of methane. Therefore, the region at low temperature in the profile of water formation could be attributed to the reduction of MoO_3 to MoO_2 with different particle size, whereas the water formation at high temperature (above 500 °C) is likely due to the formation of Mo

carbide. Then, the TPC experiments suggests that Mo carbide was formed after treatment at 650 °C for 2h under 20 % CH_4/H_2 (v/v) mixture for all samples. XRD experiments after TPC were carried out to confirm the formation of Mo carbide phase and the results will be presented next.

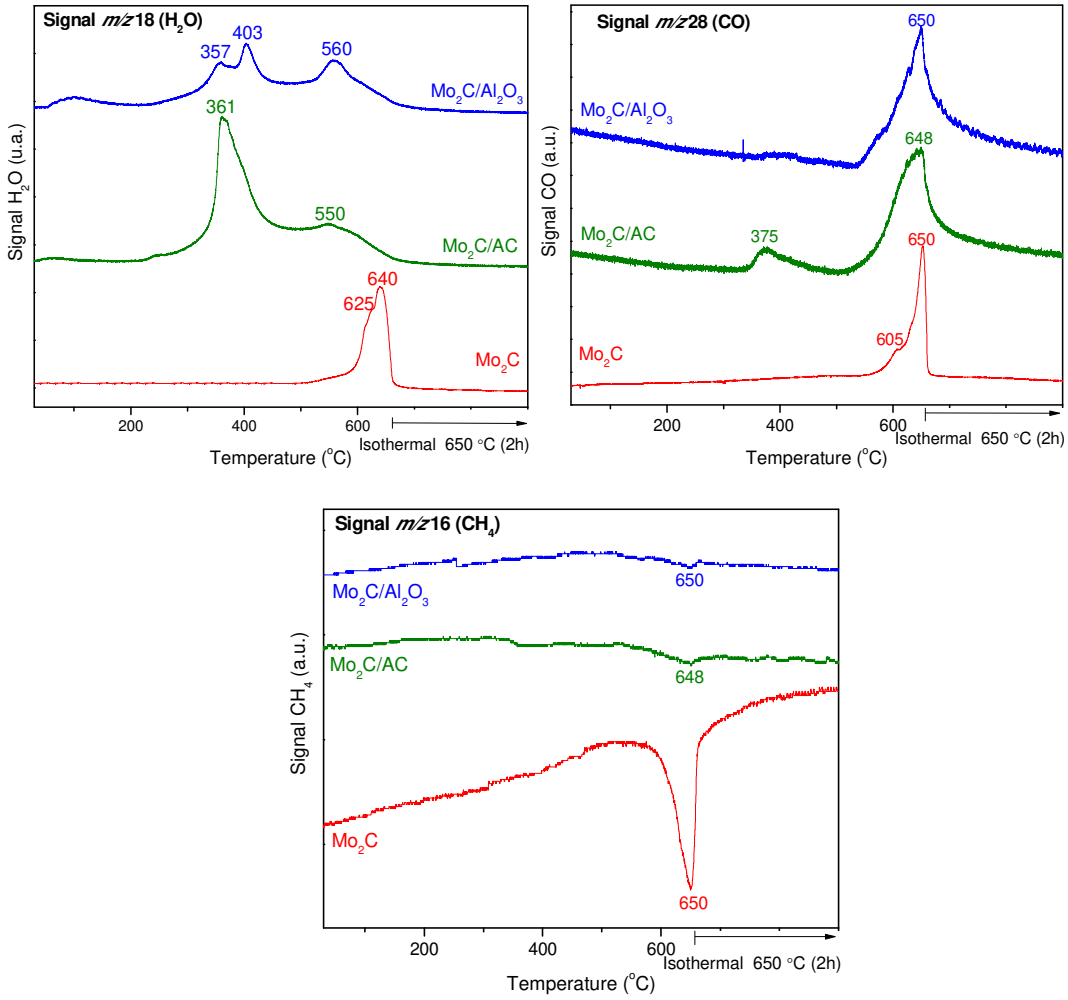

Figure 1. Signals of the products formed during the TPC up to 650 °C (2.5 °C min^{-1}) under 20 % CH_4/H_2 (v/v) mixture. *m/z* 18 (H_2O); *m/z* 28 (CO); and *m/z* 16 (CH_4).

Fig. 2 shows the diffractograms of Mo-based catalysts after carburization. The diffractogram of bulk Mo_2C exhibits the lines characteristic of β-Mo_2C phase (ICDD 35-0787) at 2θ = 34.4, 37.9, 39.4, 52.0, 61.7, 69.5, 72.4, 74.6 and 75.5°. However, the

lines corresponding to MoO_3 (2θ = 12.8, 25.7, 39.0°) phase are also observed, suggesting that the Mo carbide was partially oxidized when the sample was exposed to air after TPC. However, this phase is not expected during the catalytic experiment because the catalyst was in situ reduced before the reaction.

For both supported catalysts, the diffractograms revealed the presence of the main diffraction line of β-Mo_2C phase at 2θ = 39.4°, which agrees well with the TPC results that revealed the formation of carbide phase.

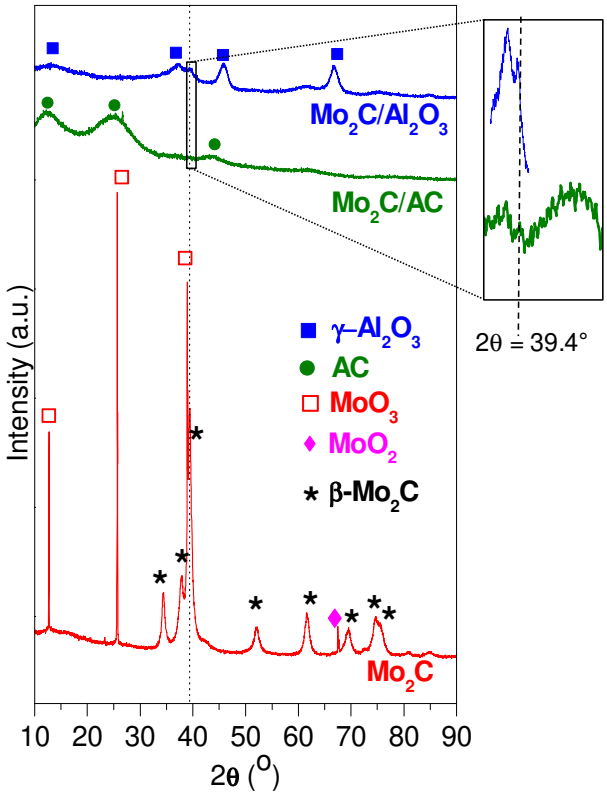

Figure 2. X-ray diffractograms of Mo_2C, Mo_2C/AC and Mo_2C/Al_2O_3 samples. Dotted line corresponds to the most intense diffraction line of β-Mo_2C phase (2θ = 39.4°).

It has been observed that the type of support influences the formation of molybdenum carbide phase. Han *et al.* [34] reported the formation of the molybdenum

carbide phase on carbon nanotube (CNT) at lower temperature than over activated carbon support.

The amount of CO chemisorbed and the calculated dispersion are reported in Table 1. Both supported Mo_2C catalysts have approximately the same dispersion around 14-15 %, which is in agreement with other works in the literature [24,35].

Table 1. CO chemisorption and carbide dispersion (D).

Catalyst	Chemisorption ($\mu mol_{CO} \cdot g_{catalyst}^{-1}$)	D (%)
Mo_2C	68	-
Mo_2C/AC	141	14.4
Mo_2C/Al_2O_3	150	15.3

3.2. Catalytic fractionation of sugarcane bagasse

First, the delignification of sugarcane bagasse was performed using the *Organosolv* treatment in an aqueous solution containing 2-propanol (iPrOH:H_2O, 70 % v/v) at 180 °C for 3 h. 2-Propanol was used as a solvent as well as a hydrogen-donor. The aim of this procedure is to retain the holocellulose (cellulose and hemicellulose) fraction as a solid residue and to keep the lignin in the liquid phase.

After treatment with aqueous solution of isopropanol (iPrOH), 30 % of the initial biomass produced the bio-oil and 70 % was recovered as the solid residue (pretreated bagasse) (Table 2). The relative content of cellulose in the pretreated bagasse increased from 39.9 % (untreated bagasse) to 52.8 % (pretreated bagasse), while the hemicellulose fraction remained unchanged around 25 % (Table S1). Based on the initial content, this treatment retained a considerable part of the sugars in the solid residue with high

411 recovery of cellulose (93 %) while hemicellulose was partially recovered (69 %) (Table
412 2). However, the insoluble lignin content decreased considerably from 22.5 to 13.1%
413 (Table S1), resulting in 59 % of delignification of sugarcane bagasse (Table 2).

414

415 **Table 2.** Degree of delignification and recovered fraction (%) after *Organosolv* reaction
416 with isopropanol solution in the absence of catalyst (iPrOH) and in the presence of
417 Raney-Ni (Ni+iPrOH), Mo_2C (Mo_2C+iPrOH), Mo_2C/AC (Mo_2C/AC+iPrOH) and
418 Mo_2C/Al_2O_3 (Mo_2C/Al_2O_3+iPrOH) catalysts.

	iPrOH	**Ni+iPrOH**	**Mo_2C+iPrOH**	**Mo_2C/AC+iPrOH**	**Mo_2C/Al_2O_3+iPrOH**
Bio-oil fraction	30	23	49	34	45
Solid fraction	70	69	44	36	47
Fraction sum	100	92	92	70	92
Delignification	59	62	80	14	14
Recovered fraction in pretreated bagasse in comparison to the initial biomass *(%, m/m)					
Cellulose	93	93	73	31	28
Hemicellulose	69	74	28	15	31

* Untreated bagasse consisted of 39.90 % cellulose, 25.69 % hemicellulose, 22.54 % total lignin, 4.96 % extractives and 0.93 % ash (Table S1).

419

420 A similar result was reported by Novo *et al.* [36] for *Organosolv* fractionation of
421 sugarcane bagasse with an aqueous solution containing 80 % of glycerol. The authors
422 recovered 93 % of cellulose, a value similar to the one obtained in our work with iPrOH
423 reaction, and approximately 80 % of delignification was achieved at 190 °C and 4 h.
424 The lower degree of delignification of our work is likely due to the type of solvent and
425 the lower reaction temperature used (2-propanol, 180 °C). Ferrini and Rinaldi [10] used
426 the *Organosolv* method for the delignification of poplar wood under the same
427 conditions of our work (reaction temperature and solvent) and obtained 77 % of

428 delignification. This result reveals the effect of the composition of lignocelullosic
429 biomass on the delignification degree. Lignin from grasses, such as sugarcane bagasse,
430 is less susceptible to delignification than lignin from hardwood (poplar). The reactivity
431 of lignin depends on the composition of reactive functional groups within monomer
432 units [37]. Lignin is composed by three fundamental monomers: *p*-coumaryl alcohol (*p*-
433 hydroxyphenol - H), coniferyl alcohol (guaiacyl - G), and sinapyl alcohol (syringyl - S).
434 In softwood lignins, the dominant monomer is guaiacyl (G), while hardwood lignins
435 consists of both guaiacyl (G) and syringyl (S) units. Grasses have large quantities of all
436 three phenylpropylenes [38].

437 Van den Bosch *et al*. [39] performed the catalytic fractionation of different
438 lignocellulosic feedstocks (birch, poplar, a pine-spruce mixture and *Miscanthus*) using
439 the *Organosolv* method with methanol and H_2 for 3 h and a Ru/C catalyst. The
440 hardwoods (birch and poplar) exhibited both the highest degree of delignification (93 %
441 and 86 %, respectively), and the highest yields of monomers and dimers. On the other
442 hand, the softwood samples (pine and spruce mixture) led to a moderate degree of
443 delignification (56 %) and a low yield of phenolic monomers. *Miscanthus* samples,
444 which belongs to the family of grasses as sugarcane bagasse, presented an intermediate
445 degree of delignification (63 %), as well as an intermediate monomer yield. Therefore,
446 these results indicate that the lignin building block composition will influence in its
447 tendency to depolymerization into phenolic monomers and dimers compounds.

448 Fig. 3 shows a two-dimensional gas chromatography (GC×GC-TOFMS) image
449 corresponding to the bio-oil obtained by the *Organosolv* treatment of sugarcane bagasse
450 without catalyst, highlighting the main detected and identified species.

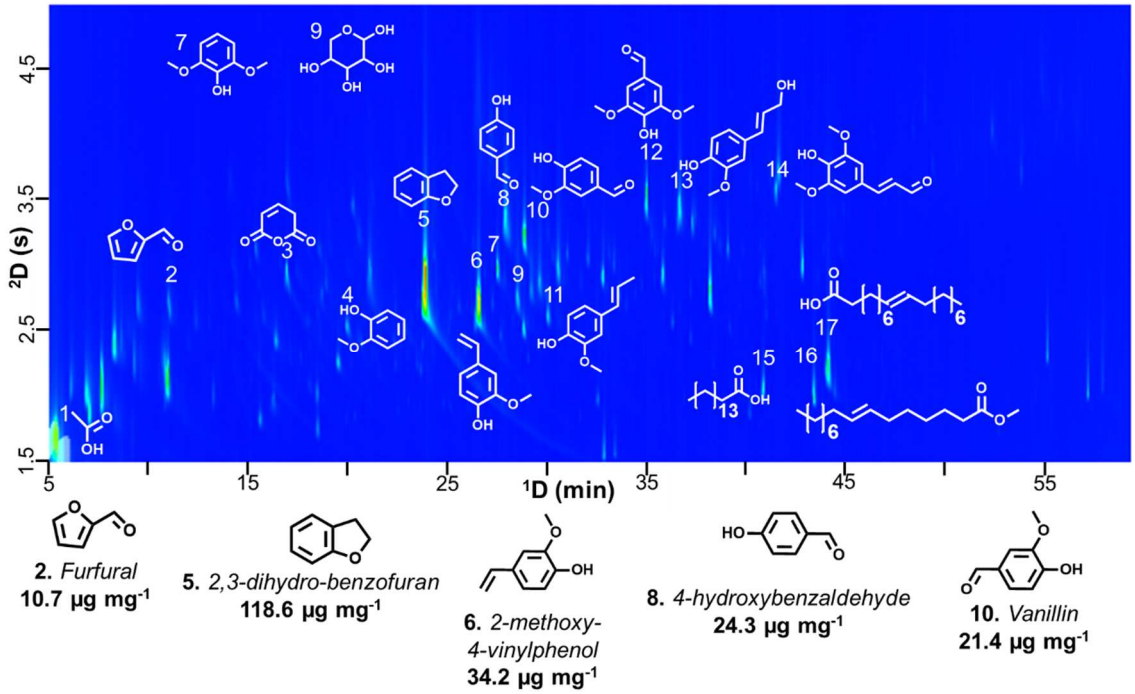

Figure 3. GC×GC-TOFMS chromatogram of bio-oil sample from iPrOH *Organosolv* treatment. The main analytes are highlighted under the chromatogram.

2,3-dihydrobenzofuran is the main component of the bio-oil (118.6 µg mg^{-1}) that also contains significant amounts of substituted methoxyphenols (2-methoxy-4-vinylphenol, vanillin, 4-hydroxy-benzaldehyde). 2,3-dihydrobenzofuran and substituted methoxyphenols are obtained from the decomposition of lignin structure [40,41]. Phenylcoumaran structures formed by β-5´ coupling are one of the main structures present in the lignin of sugarcane bagasse as identified in the NMR (Nuclear Magnetic Resonance) spectra [42]. The depolymerization of this structure led to the formation of 2,3-dihydrobenzofuran (Fig. 4), which has pharmaceutical, industrial, and medical applications. Several biologically active natural and synthetic compounds are based on the 2,3-dihydrobenzofuran core. For instance, 2,3-dihydrobenzofurans have antitubercular, anti-HIV, anticancer, antiprotozoal and cytotoxic activities [43].

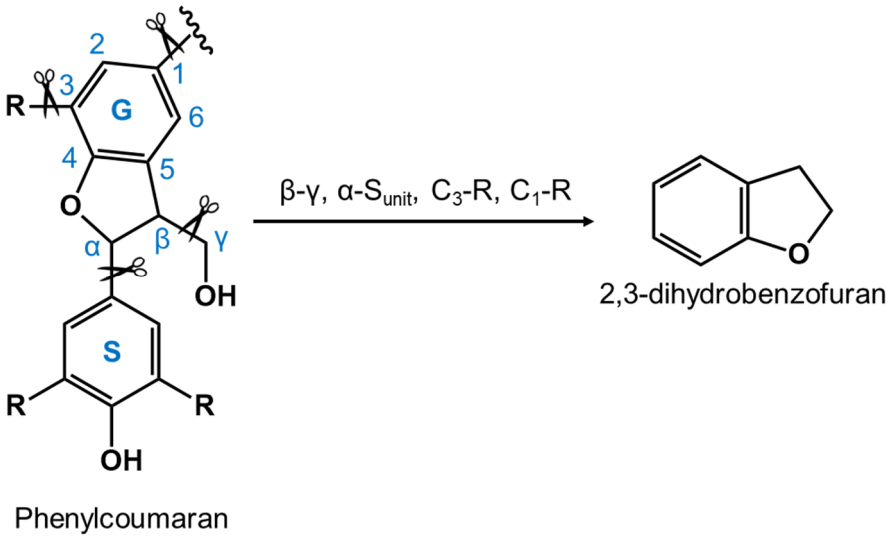

467

468 **Figure 4.** Depolymerization of phenylcoumaran structures and formation of 2,3-
469 dihydrobenzofurans, where, G: guaiacyl and S: syringyl units; C_1 and C_3 are the carbons
470 in position 1 and 3, respectively, of the guaiacyl units.

471

472 GC×GC images of the bio-oil obtained by *Organosolv* treatment of poplar wood
473 under the same reaction conditions used in our work (180 ^{o}C, iPrOH/H_2O (7:3, v/v))
474 [10] did not reveal the presence of 2,3-dihydrobenzofuran, which also demonstrate that
475 this compound is typical of depolymerization of lignin derived from grasses.

476 Table 3 reports the concentration of the main classes of compounds present in
477 the bio-oil. Substituted phenols and methoxyphenols stood out as a class of compounds
478 identified in the bio-oil (44.7 %) and they are derived from lignin. Table S2 lists the
479 main constituents of the bio-oil obtained without catalyst and their respective
480 concentrations. Substituted methoxyphenols such as 2-methoxy-4-vinylphenol (analyte
481 6, Fig. 3) was detected. This compound has application as flavoring agent in foods and
482 beverages [44]. Additionally, a considerable amount of vanillin was quantified, which is
483 a lignin oxidation product applied as flavoring agent for foods [45].

484

485 **Table 3.** Concentration (μg $mg_{biooil\text{-}volatilized}^{-1}$) and percentage of the identified classes in
486 the bio-oils obtained by Semi-quantification via GC×GC-TOFMS. Fraction of volatiles
487 at 300 °C obtained by thermogravimetric analysis of bio-oils.

Group**	Concentration (μg $mg^{-1}_{biooil\text{-}volatilized}$* / %)									
	iPrOH		**Ni+iPrOH**		**Mo_2C+iPrOH**		**Mo_2C/AC+iPrOH**		**Mo_2C/Al_2O_3+iPrOH**	
Carbohydrates derived-compounds										
Acids	5.5	/1.9	21.2	/2.7	12.4	/4.1	19.1	/3.9	9.0	/2.8
Alcohols and sugars	7.0	/2.5	73.7	/9.5	13.9	/4.5	23.4	/4.8	11.6	/3.7
Ketones	0.6	/0.2	0.5	/0.1	2.5	/0.8	5.7	/1.2	7.0	/2.2
Esthers	2.0	/0.7	1.0	/0.1	4.7	/1.5	26.2	/5.3	2.8	/0.9
Furanics derived	18.8	/6.6	237.2	/30.6	45.9	/15.0	76.4	/15.6	109.7	/34.7
Lignin derived-compounds										
Substituted phenols and methoxyphenols	126.8	/44.7	146.3	/18.9	107.2	/35.0	208.1	/42.4	129.0	/40.8
2,3-Dihydrobenzofuran	118.6	/41.8	3.6	/0.5	118.2	/38.6	121.8	/24.8	1.2	/0.4
Others lignin derived-compounds	3.5	/1.2	289.8	/37.4	1.6	/0.5	9.8	/2.0	45.8	/14.5
Hydrocarbons	0.9	/0.3	2.5	/0.3	0.1	/0.0	0.0	/0.0	0.3	/0.1
Total	283.7		776.2		306.5		490.5		316.3	
Fraction volatiles 300 °C (%)	54		76		39		48		54	

* Concentration: semi-quantified analyte mass relative to bio-oil volatilized mass at 300 °C

** Aldehydes and ethers were found in traces in the bio-oil samples

488

489 The *Organosolv* treatment was also evaluated in the presence of Raney-Ni
490 commercial catalyst, used as reference, in comparison to molybdenum carbide catalysts,
491 proposed in our study as alternative catalyst. The addition of Raney-Ni catalyst did not

492 produce significant changes in the delignification degree (62 %) or in the fraction of
493 recovered cellulose (93 %) and hemicellulose (74 %) in the solid residue (Table 2) in
494 comparison to the *Organosolv* treatment without catalyst. The variations in the relative
495 content of cellulose, hemicellulose and lignin in the solid residue were also quite close
496 to the ones observed in the absence of catalyst (Table S1).

497 Van den Bosch *et al.* [19] reported similar results with the *Organosolv* treatment
498 of birch sawdust using methanol and Ni/Al_2O_3 catalyst, reaching delignification degrees
499 of 84 and 87 % without and with catalyst, respectively. According to the authors, the
500 solvent was responsible for the extraction of lignin and its subsequent depolymerization
501 by solvolytic cleavage of the β-O-4 bonds. It was suggested that the catalyst stabilized
502 the products generated from lignin, preventing the repolymerization. The ability of
503 organic solvents to dissolve lignin facilitates its depolymerization especially because of
504 the increase in mass transfer between the catalyst and solubilized substrate [6]. In
505 contrast, for the wood poplar, Ferrini and Rinaldi [10] reported a decrease in the
506 delignification degree on the treatments in the presence of Raney-Ni catalyst (77 to 63
507 %).

508 The chromatogram of the bio-oil produced in the presence of Raney-Ni catalyst
509 is displayed in Fig. 5. The presence of acetic acid and diols corresponds to the
510 depolymerization of cellulose and hemicellulose. In addition, Fig. S1 shows that at least
511 76 % of the compounds present in the Ni+iPrOH bio-oil are volatilized at 300 °C
512 (temperature of chromatograph injector), and therefore analyzed. It is important to take
513 into account that this was the bio-oil sample with the highest fraction of volatiles, with
514 775.8 μg of analytes identified for each mg of volatilized bio-oil (at 300 °C, Table 3).
515

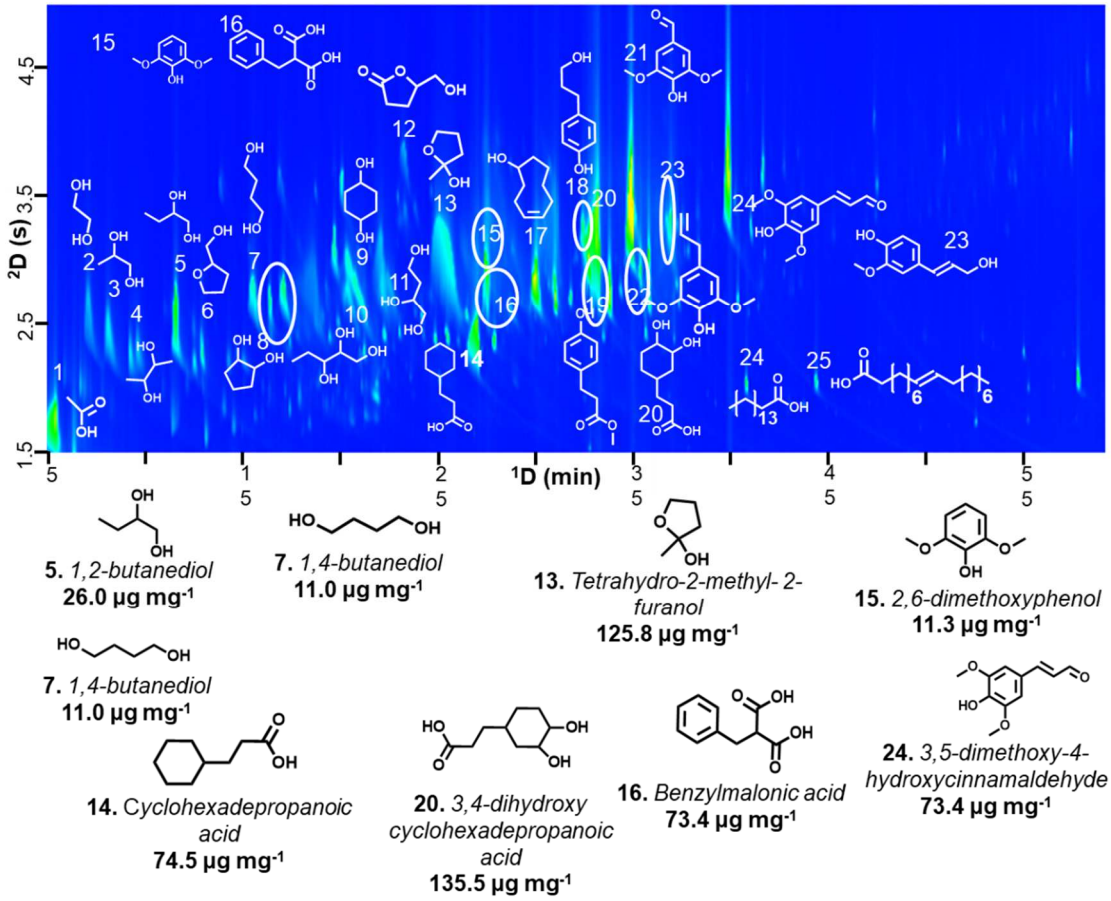

Figure 5. GC×GC-TOFMS chromatogram of bio-oil sample from Ni+iPrOH catalyzed iPrOH *Organosolv* treatment. The main analytes are highlighted under the chromatogram.

As show in Tables 3 and S2, the bio-oil obtained from the *Organosolv* treatment in the presence of Raney-Ni catalyst contained larger amounts of acids (acetic acid), alcohols (1,2-butanediol and 1,4-butanediol), furans (tetrahydro-2-methyl-2-furanol) and lactones (2-hydroxy-γ-butyrolactone and 5-hydroxymethyldihydrofuran-2-one) than the treatment with only iPrOH without catalyst. 5-Hydroxymethyldihydrofuran-2-one is a product of hydrogenation of the ring of 5-Hydromethyl-2(5H)-furanone (HBO), an important feedstock for the production of different antimumor, antibacterial, antiviral drugs such as azidotimidine (AZT) and Remdesivir that is used in the treatment of

529 coronavirus disease 2019 (COVID 19) [46]. Acetic acid is likely due to sugars
530 degradation and acetyl bond cleavage in the xylans [47].

531 The main lignin-derived products formed were 3,4-dihydroxy-
532 cyclohexanepropanoic acid (135.3 μg/mg), 3-(4-hydroxy-3,5-dimethoxyphenyl)-prop-2-
533 enal (72.4 μg/mg), cyclohexanepropanoic acid (74.5 μg/mg), and benzylmalonic acid
534 (73.4 μg/mg). Curiously, only a low concentration of 2,3-dihydrobenzofuran was
535 detected in the bio-oil obtained in the presence of Raney-Ni (3.6 μg/mg).
536 Benzylmalonic acid was not produced in the absence of the catalyst and 3-(4-hydroxy-
537 3,5-dimethoxyphenyl)-prop-2-enal was produced in low concentration, indicating that
538 Raney-Ni participated on the depolymerization of lignin and then, changed the product
539 distribution. 3,5-Dimethoxy-4-hydroxycinnamaldehyde (sinapaldehyde) is an
540 intermediate in the synthesis pathway of native lignin monomer precursor sinapyl
541 alcohol [4].

542 Comparing the Ni+iPrOH bio-oil from sugarcane bagasse with that from wood
543 [10], both exhibited high content of alcohols from hydrogenolysis of hemicellulose
544 sugars [47]. Analyzing qualitatively, the bio-oil obtained from the treatment of wood
545 with Raney-Ni catalyst presented mostly methoxyphenols similar to the ones presented
546 in the sugarcane bio-oil, such as eugenol, 2,6-dimethoxyphenol, 2,6-dimethoxy-4-(2-
547 propenyl)-phenol. However, the bio-oil from sugarcane differ from that of wood by the
548 presence of phenol and methoxyphenols substituted by acid groups (analytes 14, 16 and
549 20, Fig. 5).

550 *Organosolv* treatment of bagasse was also evaluated in the presence of
551 molybdenum carbide catalysts (bulk Mo_2C or Mo_2C supported on activated carbon
552 (AC) or γ-Al_2O_3).

553 The treatment with the bulk Mo_2C catalyst (Mo_2C+iPrOH) produced a larger
554 amount of bio-oil and, consequently, a decrease in the solid fraction was observed,
555 when compared to the reactions with only iPrOH or Ni+iPrOH (Table 2). This is likely
556 due to the higher delignification degree (80 %) as well as to the larger extent of
557 cellulose and hemicellulose depolymerization. At this condition, only 28 % of the
558 hemicellulose of the untreated bagasse was retained in the solid residue. This affected
559 the bio-oil composition that contained acetic acid (11.8 μg/mg), xylose (9.3 μg/mg),
560 furfural (17.3 μg/mg) and furan (7.9 μg/mg), all hemicellulose-derived products (Table
561 S2). However, diols and triols were not formed.

562 Fig. 6 shows the chromatogram of the bio-oil produced in the treatment with the
563 bulk Mo_2C catalyst. There was practically no formation of diols in the bio-oil produced
564 by bulk Mo_2C that also exhibited a lower formation of acetic acid than Raney-Ni (Table
565 S2). On the other hand, xylose, furfural and furan were preferentially formed on the
566 carbide-based catalyst (Table S2). The concentration of substituted phenols and
567 methoxyphenols (107.2 μg/mg) was lower than on Raney-Ni (Table 3). The main
568 compound in the bio-oil obtained from the treatment with Mo_2C was 2,3-
569 dihydrobenzofuran (118.2 μg/mg), as observed for the *Organosolv* reaction without
570 catalyst. Moreover, 2-methoxy-4-vinylphenol (34.5 μg/mg), 4-hydroxybenzaldehyde
571 (19.3 μg/mg), vanillin (16.5 μg/mg), and 4-hydroxy-3,5-dimethoxybenzaldehyde (10.1
572 μg/mg) were also detected (Table S2).
573

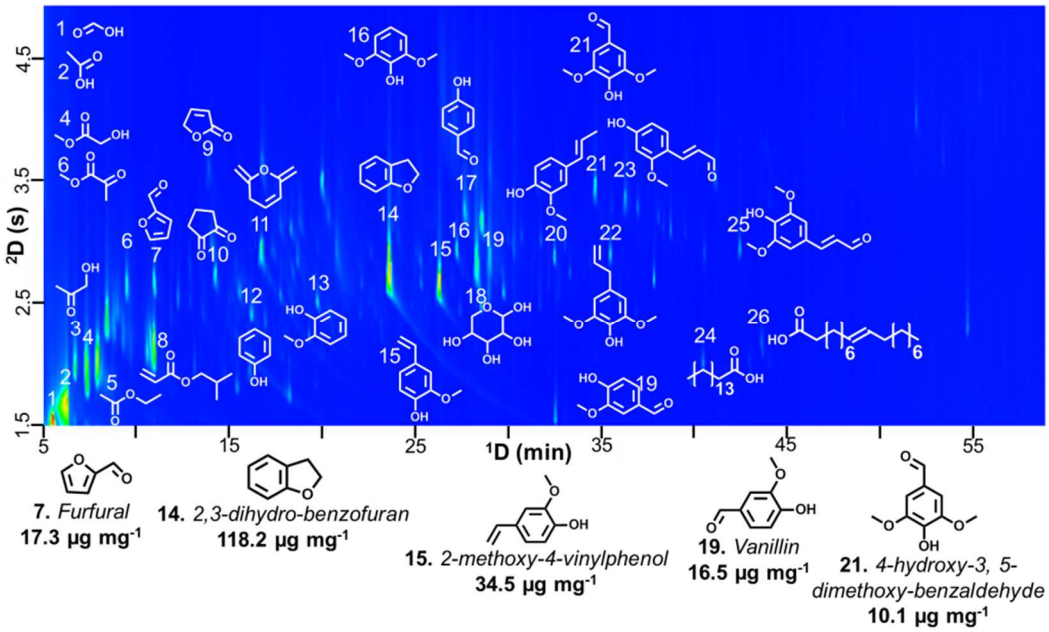

574

575 **Figure 6.** GC×GC-TOFMS chromatogram of bio-oil sample from bulk Mo_2C catalyzed
576 iPrOH *Organosolv* treatment. The main analytes are highlighted under the
577 chromatogram.

578

579 It is also important to notice that only 39 % of the bio-oil obtained on the
580 treatment with bulk Mo_2C was volatized at 300 °C (temperature of chromatograph
581 injector) as shown by the TGA experiments (Fig. S1), which may explain the apparent
582 decrease in the total amount of compounds in this bio-oil, when compared with the bio-
583 oil from Ni+iPrOH catalyzed system.

584 In comparison to the reaction with bulk Mo_2C reaction, the use of Mo_2C
585 supported in AC or Al_2O_3 resulted in low delignification (14 %) and high cellulose and
586 hemicellulose extraction. For instance, it was observed a retention of only 31 and 15 %
587 of the initial cellulose and hemicellulose content, respectively, in the solid residue
588 recovered after the reaction with Mo_2C/AC (Table 2). These results agree with the
589 considerable amount of acetic acid, xylose, furfural and lactones in the bio-oils from
590 reactions catalyzed by Mo_2C supported catalysts (Table S2).

591 The bio-oil produced in the treatment with Mo_2C/AC (Fig. 7) contained
592 considerable amounts of acetic acid (18.7 μg/mg), xylose (18.2 μg/mg) and furfural
593 (29.2 μg/mg) (Table S2). These results show a significant depolymerization of
594 hemicellulose in the presence of Mo_2C/AC catalyst. 2,3-Dihydrobenzofuran was the
595 main lignin derived product (121.8 μg/mg) as observed for the bulk Mo_2C catalyst.
596 Considering the substituted phenols and methoxyphenols, there was significant
597 formation of 2-methoxy-4-vinylphenol (51.5 μg/mg), 4-hydroxy-benzaldehyde (30.5
598 μg/mg), 2,6-dimethoxy-4-(2-propenyl)-phenol (24.5 μg/mg), 4-hydroxy-3,5-dimethoxy-
599 benzaldehyde (15.7 μg mg^{-1}) and 2-methoxy-4-(1-propenyl)-phenol (15.4 μg mg^{-1}). The
600 Mo_2C/Al_2O_3+iPrOH bio-oil (Fig. 8) contained a significant amount of lactones such as
601 2-hydroxy-γ-butyrolactone and substituted methoxyphenols such as 3-hydroxy-4-
602 methoxy-benzaldehyde. As observed for Raney-Ni catalyst, 2,3-dihydrobenzofuran was
603 not formed in the reaction using Mo_2C/Al_2O_3 catalyst. The tests with Mo_2C/AC and
604 Mo_2C/Al_2O_3 catalysts exhibited the highest yield to substituted methoxyphenols (24 %),
605 which, in general, are good octane components of gasoline.
606

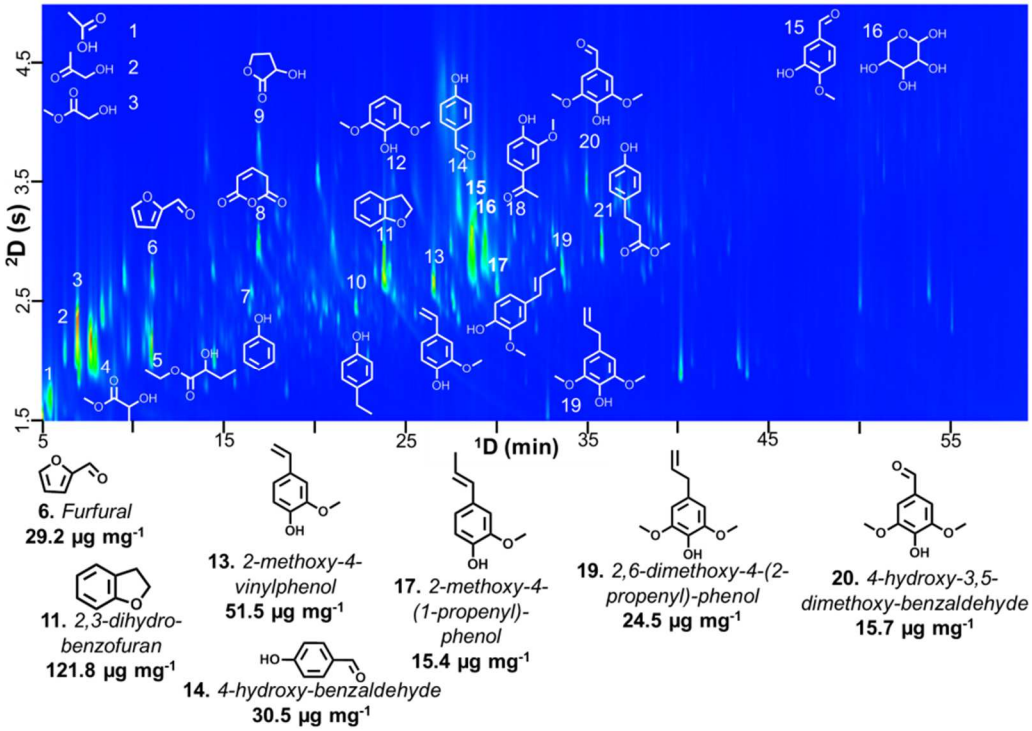

607

608 **Figure 7**. GC×GC-TOFMS chromatogram of bio-oil sample from Mo_2C/AC catalyzed
609 iPrOH *Organosolv* treatment. The main analytes are highlighted under the
610 chromatogram.

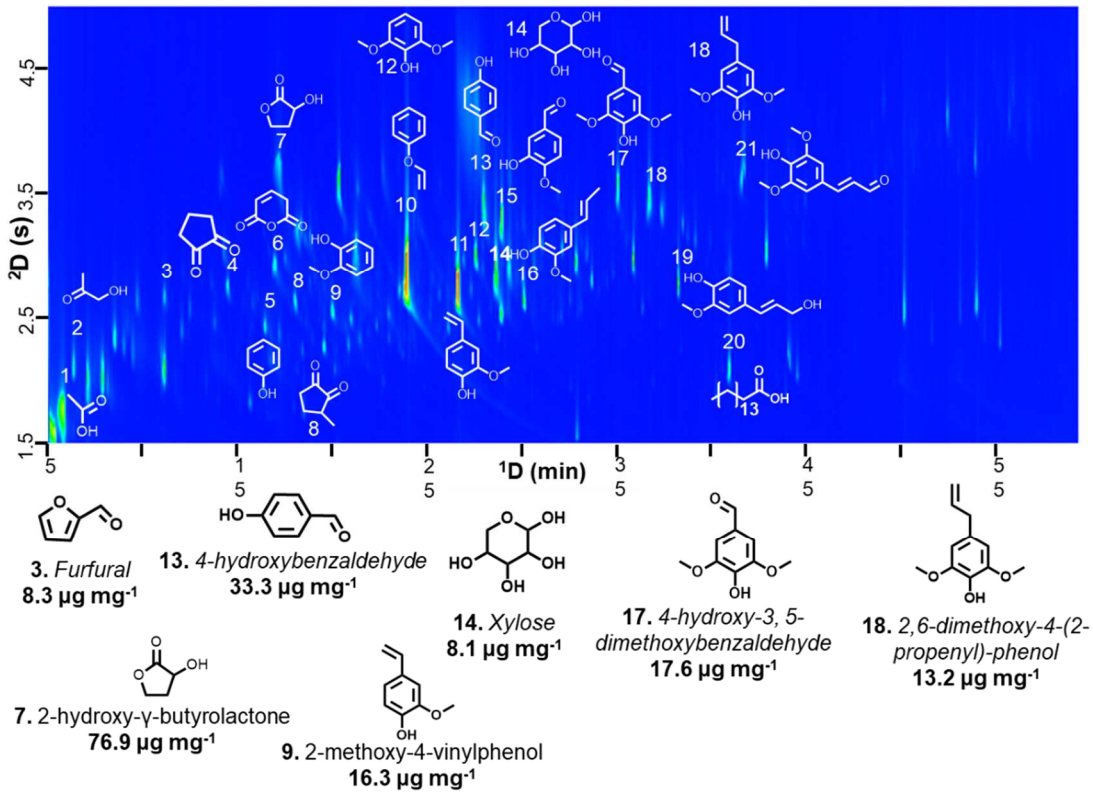

Figure 8. GC×GC-TOFMS chromatogram of bio-oil sample from Mo_2C/Al_2O_3 catalyzed iPrOH *Organosolv* treatment. The main analytes are highlighted under the chromatogram.

3.3. Effect of the type of metal phase

The fractionation of sugarcane bagasse caused a partial extraction of hemicellulose from the biomass through the solvolysis performed by the isopropanol/water mixture, whereas the cellulose fraction remained in the solid residue practically untouched. The addition of Raney-Ni did not change significantly the fraction of cellulose and hemicellulose recovered in the solid residue in comparison the *Organosolv* treatment of bagasse. However, in the presence of Raney-Ni catalyst, the solvolytic extraction of hemicellulose was accompanied by its catalytic depolymerization and the formation of large quantities of diols (1,2-butanediol, 1,4-butanediol), triols (glycerol, 1,2,4-butanetriol), furans (tetrahydro-2-methyl-2-furanol) and lactones (2-hydroxy-γ-butyrolactone and 5-hydroxymethyldihydrofuran-2-one). The

626 carbide phase also favored the depolymerization of hemicellulose, but the main products
627 obtained were xylose and furfural.

628 Hemicelluloses are linear polymers of β-D-xylopyranosyl units linked by (1→4)
629 glycosidic bonds (xylose), with many of the xylose units substituted at position 2 or 3
630 by 4-O-methyl-α-D-glucuronopyranosyl acid. Hemicelluloses may also have a high rate
631 of substitution by acetyl groups. In the presence of catalysts, the amount of acetic acid,
632 diols, xylose, furfural and lactones in the bio-oil significantly increased (Table S2).
633 These results indicates that they catalyzed the removal of the acetyl groups and the
634 acetic acid released likely promoted the cleavage of β-(1,4) glycosidic bonds of
635 hemicellulose. The xylose formed is isomerized and dehydrated to furfural [48], or it is
636 hydrogenated to xylitol [49] (Scheme 2). The dehydration is promoted by the acid sites
637 of the supported Mo_2C catalysts represented by the Lewis acid sites of the support
638 (alumina) and of the Mo_2C phase. This explains the higher fraction of furfural on the
639 bio-oil of Mo_2C based catalysts. On the other hand, Raney-Ni does not contain acidity
640 and then, this reaction pathway is not relevant. However, this catalyst has high
641 hydrogenation and hydrogenolysis activity. Therefore, glucose and xylose are
642 preferentially hydrogenated to sorbitol and xylitol, respectively. The hydrogenolysis of
643 sorbitol and xylitol leads to the production of glycerol, ethylene glycol and 1,2,3-
644 butanetriol that is further converted to 1,2-butanediol or 1,4-butanediol [50]. The
645 dehydrogenation of 1,4-butanediol may produce γ-butyrolactone and its derivatives.
646 Therefore, the active phase (metallic Ni or Mo2C) and the type of support strongly
647 affects the product distribution of the bio-oil.
648

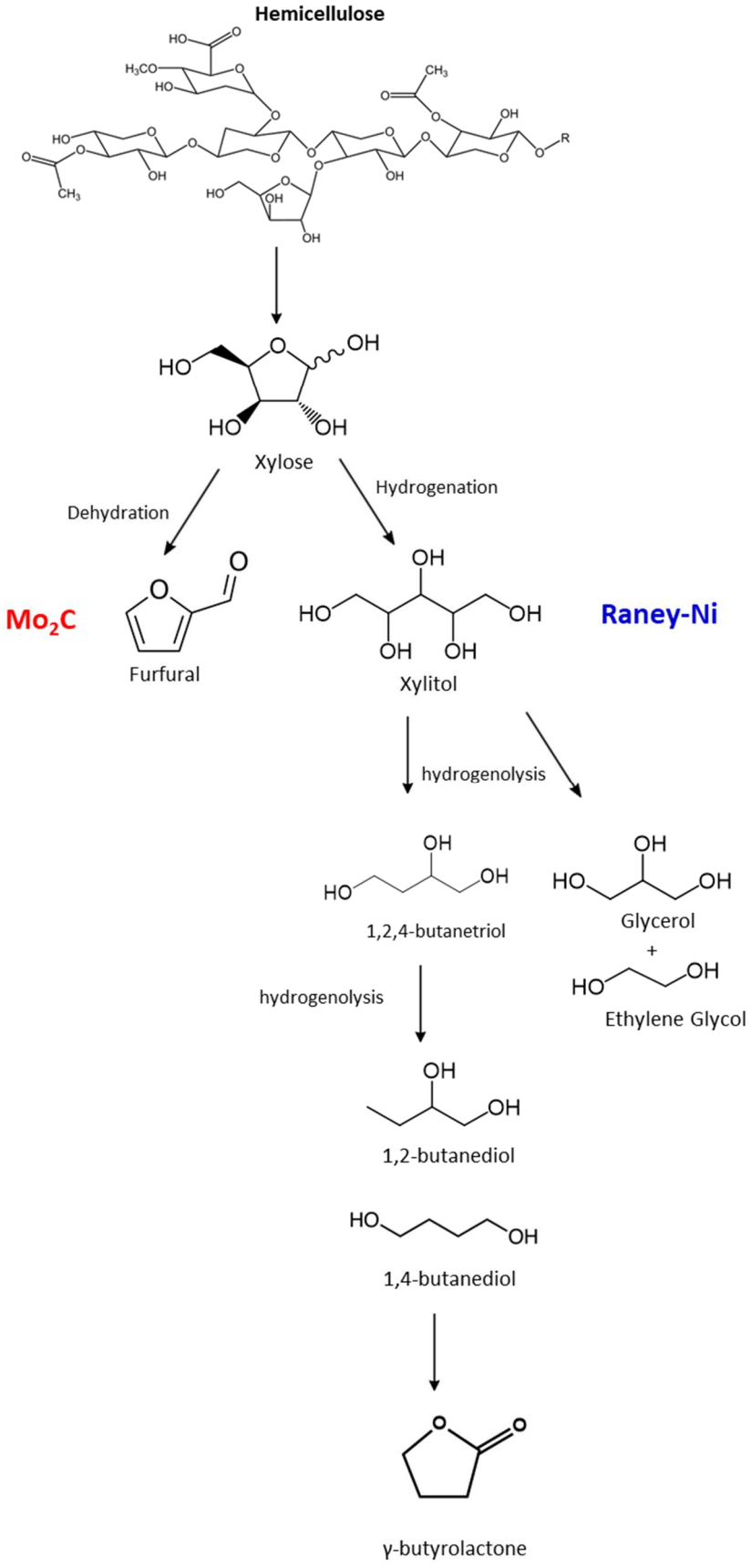

649

650 **Scheme 2.** Reaction pathways for the production of the main hemicellulose-derived
651 products observed in this work on Raney-Ni and Mo_2C-based catalysts.

The addition of catalyst also affected the product distribution obtained from lignin depolymerization, which depended on the active phase (Fig. 9). For *Organosolv* treatment, 2,3-dihydrobenzofuran was the main product formed, while Raney-Ni catalyst favored the formation of 3,4-dihydroxy-cyclohexanepropanoic acid, cyclohexanepropanoic acid and benzylmalonic acid, substituted methoxyphenols that were only formed on this catalyst.

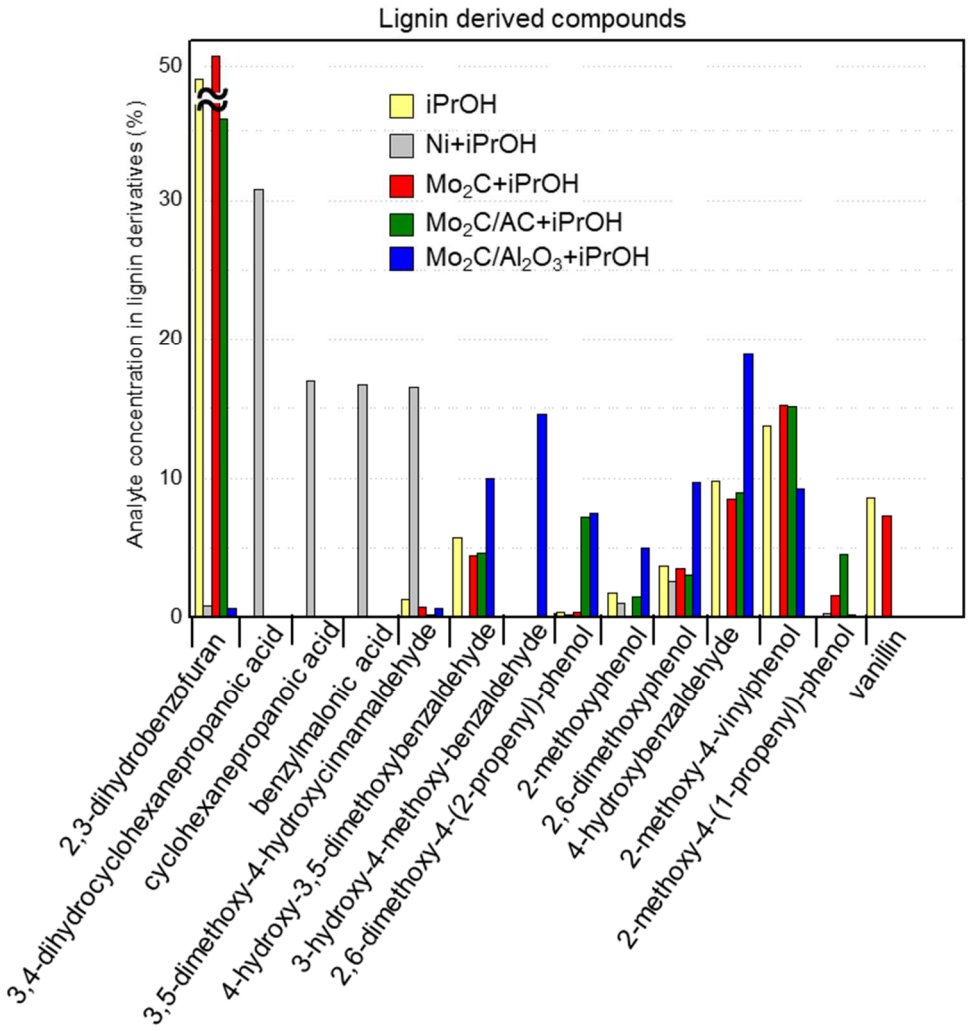

Figure 9. Distribution of the concentration of main identified analytes derived from lignin. Percentage calculated in relation to the total products derived from lignin.

For the bulk Mo_2C catalyst, the product distribution and the percentage of lignin-derived compounds was quite similar to that for *Organosolv* treatment without catalyst. However, the percentage of each lignin-derived compounds varied on the supported carbide phase in comparison to the *Organosolv* treatment without catalyst. For instance, 3-hydroxy-4-methoxybenzaldehyde and 2,6-dimethoxy-4-(2-propenyl)-phenol were formed over Mo_2C/Al_2O_3 catalyst, but they were not observed in the bio-oil of the *Organosolv* treatment without catalyst. For Mo_2C/AC catalyst, 2,6-dimethoxy-4-(2-propenyl)-phenol, and 2-methoxy-4-(1-propenyl)-phenol were formed whereas only trace amounts were detected in the *Organosolv* treatment without catalyst. These results revealed that the type of support also plays a role in the reaction since the carbide phase was the same, regardless the catalyst.

Scheme 3 shows the main lignin structures containing different units for grasses with inter-unit bonding such as ferulate or tricin units [42]. This Scheme also displays the main compounds formed in the bio-oil obtained with the Raney-Ni and Mo_2C catalysts, representing the cleavage of different C-O and C-C bonds. For Raney-Ni, benzylmalonic acid is obtained by the cleavage of β-O-4 bonds of the ferulate unit while 3-(4-hydroxy-3,5-dimethoxyphenyl)-prop-2-enal (sinapaldehyde) is produced by breaking β-O-4 and 4-O-5 bonds of a guaiacyl unit. 3-(p-hydroxyphenyl)-1-propanol is produced from *p*-coumarate unit. In the case of Mo_2C/AC catalyst, 2-methoxy-4-vinylphenol is formed through the cleavage of β-O-4 and α-O-4 bonds between two guaiacyl units. 2,6-Dimethoxyphenol may be obtained by the cleavage of β-1 bond between a guaiacyl/syringyl unit and phenylcoumaran unit of a ferulate structure. The cleavage of β-1 bond may occur depending on the reaction conditions and catalyst used as demonstrated by the reactions using lignin model compounds [5]. Therefore, the type

of the active phase promoted the cleavage of specific C-O and C-C bonds, originating different substituted methoxyphenols.

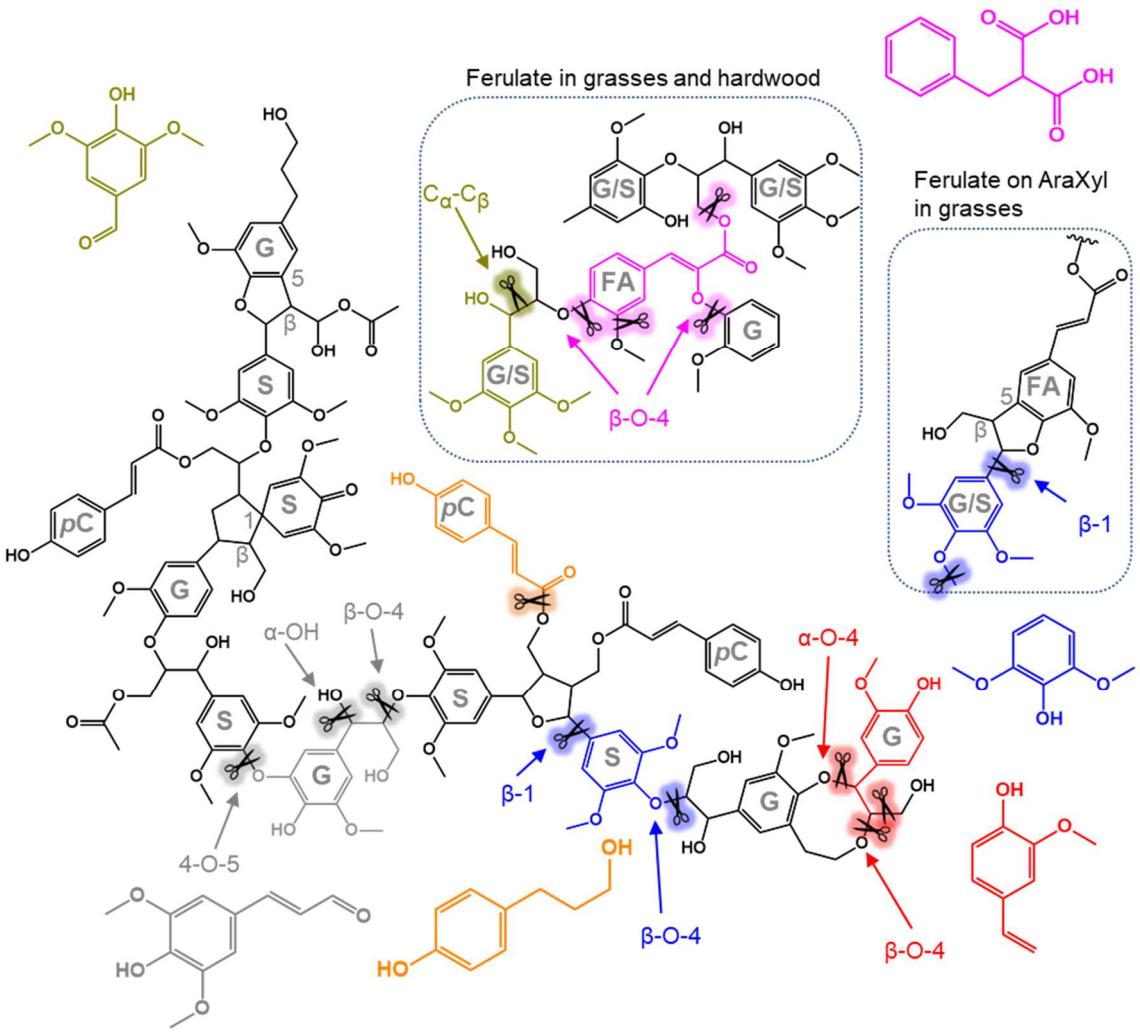

Scheme 3. Monomers formed in the reactions and suggested precursor structure. G: guaiacyl and S: syringyl units; *p*C: *p*-coumarate; FA: ferulate.

Since transition metal carbide catalysts, like the Mo_2C type catalysts presented in this work, have catalytic activity similar to noble metal catalysts [24-29], we can make a parallel with the results obtained by Ru/C catalyst used by Lv *et al*. [51]. These authors suggested a reaction mechanism for the depolymerization of a hydrolyzed residue of cornstalk chips in an aqueous solution of ethyl acetate and Ru/C catalyst. They proposed that the β-O-4, α-O-4, β-5 and 4-O-5 linkages as well as the bonds in the

700 side chain of phenylpropane (e.g., α-β, α-OH, β-OH and γ-OH) could be greatly
701 cleaved, indicating that these linkages and side chain bonds were fractured under mild
702 conditions. For instance, the β-O-4 linkages and α-β side chain bond in oligomer could
703 be broken to form dimer, and then the α-O-4 linkage and the side chain α-OH and β-OH
704 bonds in dimer might be fractured to obtain monomers. The α-O-4 and β-5 linkages of
705 dimers as well as α-OH or/and β-OH of side chain bonds, might be cleaved to obtain the
706 monomers.

707 Considering the yields of substituted methoxyphenols, Yan *et al.* [21] reported
708 the results obtained for the fractionation of birch wood sawdust in water at 200 ^{o}C and
709 40 bar of H_2 using active carbon supported Ru, Pd, Pt and Rh catalysts. The main
710 monomer formed for each catalyst were: Pt/C (guaiacylpropanol); Pd/C
711 (syringylpropanol); Rh/C (guaiacylpropanol); and Ru/C (syringylpropanol). The sum of
712 the yields of the main monomers formed followed the order: Pt/C (33.6 %) > Pd/C (25.5
713 %) > Rh/C (19.7 %) >> Ru/C (4.6 %). These results revealed that the type of the metal
714 plays a key role on the distribution of products derived from lignin depolymerization.

715 Li *et al*. [29] investigated the fractionation of birch wood at 235 ^{o}C and 60 bar of
716 H_2 in water using carbon supported W_2C promoted by Ni, Ir, Pd, Pt and Ru catalysts and
717 obtained monomers yield of 36.9, 30.6, 28.4, 26.7 and 0.00 %, respectively. In addition,
718 the distribution of phenolic products varied significantly depending on the catalyst. For
719 Pd-W_2C/AC, the main phenolic monomers were guaiacylpropanol and
720 syringylpropanol. On the other hand, Ni-W_2C/AC, Pt-W_2C/AC and Ir-W_2C/AC favored
721 the formation of guaiacylpropane and syringylpropane, which were probably produced
722 from the hydrogenolysis of guaiacylpropanol and syringylpropanol, respectively. These
723 results suggested that Pd-based catalyst favored the lignin hydrogenation preferentially
724 to hydroxyl group, while Ni-W_2C/AC and other catalysts facilitated the dehydroxylation

725 reaction. In addition, a significant formation of diols (ethylene glycol, 1,2-propylene
726 glycol, 1,2-butylene glycol) was observed for all catalysts, which was attributed to the
727 depolymerization of cellulose and hemicellulose. The yields of diols were higher than
728 that obtained for substituted methoxyphenols and followed the order: Ni-W_2C/C (70.6
729 %) > Pd-W_2C/C (47.4 %) > Pt-W_2C/AC (35.6 %) > Ir-W_2C/AC (25.2 %) > Ru-
730 W_2C/AC (0.0 %). Li *et al.* [29] also carried out the fractionation of sugarcane bagasse at
731 235 ^oC and 60 bar of H_2 on water using Ni-W_2C/C, which was the catalyst that exhibited
732 the highest yield to substituted methoxyphenols for the treatment of birch wood (36.9
733 %). The yield to substituted methoxyphenols significantly decreased to 23.4 % for the
734 treatment of sugarcane bagasse, which reveals the important effect of the biomass type
735 on the yield of substituted methoxyphenols. Furthermore, a high yield of diols was also
736 observed (59.6 %).

737 In our work, the yields of substituted methoxyphenols obtained in the
738 *Organosolv* treatment with our Mo_2C-based catalysts (bulk Mo_2C – 18 %; Mo_2C/AC -
739 24 %; Mo_2C/Al_2O_3 - 24 %) (Tab. S3) were higher than that ones for the treatment
740 without catalyst (13 %) and Raney-Ni (13 %). Considering the total yield of monomer
741 in our work, the following values were obtained for the carbide catalysts: bulk Mo_2C –
742 49 %, Mo_2C/AC - 51 %; Mo_2C/Al_2O_3 - 35 % (Tab. S3), which are comparable with the
743 data from literature for catalytic fractionation of hardwood and softwood. However, the
744 yield to monomers reported in the literature vary significantly because of the different
745 reaction conditions (temperature, pressure, solvent), catalysts and type of biomass used
746 [30], which makes the comparison of our results quite hard. In particular with sugarcane
747 bagasse, there is only the work of Li *et al*. [29] who also used supported carbide
748 catalysts. In this case, the yield to substituted methoxyphenols on both works was
749 approximately the same (23 and 24 %) but Li *et al*. [29] used more severe reaction

conditions (235 ºC and 60 bar of H_2) than our work (180 ºC and autogenous pressure). In addition, a lower formation of diols was observed in our work.

3.4. Enzymatic hydrolysis and characterization of the Organosolv pretreated bagasse

Pretreatment is one of the most expensive stages in second-generation technologies, however, it is crucial for ensuring good ultimate yields of sugars from both polysaccharides [48]. Initially, this operation has been considered a simple step, but commercial scale 2G ethanol plants presented difficulties in the treatment processes of lignocellulosic biomass [52]. Addressing this issue is fundamental for the success of the biorefinery, which allows the use of all fractions of the lignocellulosic biomass [53-55]. Therefore, it is important that both the bio-oil formed and the pretreated bagasse exhibits high quality. In this context, the enzymatic hydrolysis using cellulases of the *Organosolv* pretreated bagasse (solid residue) was performed for gaining insights into its potential as feedstock for cellulosic ethanol production.

Fig. 10 shows the glucose yield as a function of time during the enzymatic hydrolysis of the untreated and the pretreated bagasse samples obtained after the treatments with different catalysts. As expected, the untreated bagasse hydrolysis resulted in the lowest glucose yield (~ 5 %, 72 h), because cellulose in the intact plant cell walls is not promptly available for the cellulases attack. However, the hydrolysis of pretreated bagasse from the iPrOH and Ni+iPrOH treatments also achieved low glucose yields of 12 and 16 % respectively, suggesting that the modification of the cell wall structure at these conditions did not improve the exposure of cellulose for the enzymatic attack.

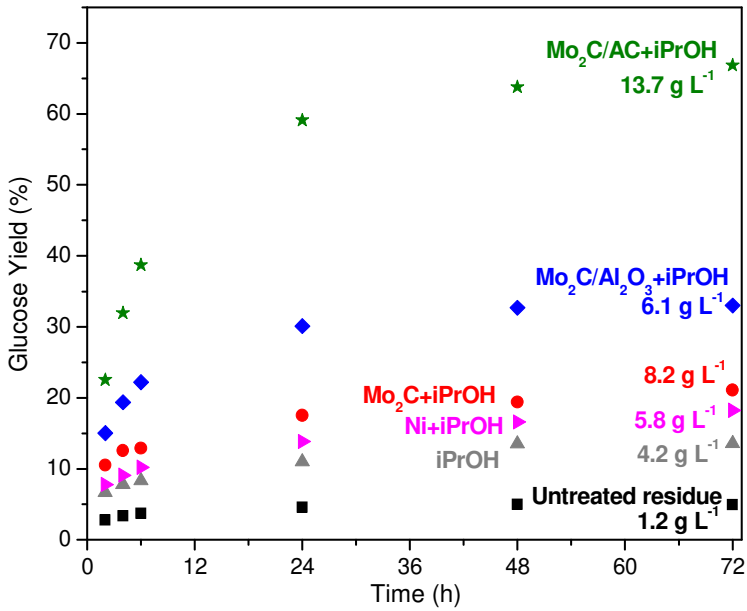

774

775 **Figure 10.** Glucose yield obtained on the enzymatic hydrolysis of untreated and
776 pretreated sugarcane bagasse after *Organosolv* treatment using isopropanol
777 (iPrOH):water solution in the absence or in the presence of different catalysts. The
778 values in $g\ L^{-1}$ refer to glucose concentration at 72 h.

779

780 Nonetheless, improved glucose yields were obtained with the pretreated biomass
781 from carbide-based catalysts treatments, corresponding to approximately 20 %, 67 %
782 and 35 % for Mo_2C, Mo_2C/AC and Mo_2C/Al_2O_3 treated samples, respectively.
783 Considering these catalysts, the highest delignification degree was obtained by the
784 treatment using Mo_2C+iPrOH, but the glucose yield was the lowest, showing that there
785 was not a direct correlation between delignification and the exposure of cellulose for the
786 enzymatic attack. This is a reasonable result, as enzymatic hydrolysis effectiveness can
787 be affected by different parameters other than lignin content, such as cellulose degree of
788 polymerization, crystallinity and hemicellulose content. For instance, the yield of
789 glucose in the enzymatic hydrolysis followed the order Mo_2C/AC > Mo_2C/Al_2O_3 >
790 Mo_2C > Raney-Ni ≈ iPrOH, which corresponded to the reverse order to the amount of
791 hemicellulose in the biomass that was hydrolyzed (Tab. S1).

Galkin *et al*. [56] performed the enzymatic hydrolysis of the pulp obtained in the treatment of different hardwoods using a Pd/C catalyst. The glucose yield for the *Organosolv* treatment without catalyst after 2 h was higher than the ones obtained for all hardwoods in the presence of Pd/C catalyst. These results indicate that the pulp obtained by the catalytic fractionation has lower susceptibility to enzymatic hydrolysis than *Organosolv* treatment and depended on the type of biomass. The glucose yield followed the order: *Organosolv* > Sweden Birch wood > Finish Birch wood > Poplar. In our work, the glucose yield obtained on the enzymatic hydrolysis of the pulp obtained by the catalytic fractionation was higher than that for *Organosolv* treatment, regardless of the catalyst.

Comparing the glucose yield and concentration obtained for the hydrolysis of Mo_2C+iPrOH pretreated bagasse with that one for Mo_2C/Al_2O_3 pretreated bagasse, it is observed that the hydrolysis of the solid residue obtained with alumina supported catalyst resulted in a higher yield, but in a lower concentration of glucose generated. The higher yield occurred because the Mo_2C/Al_2O_3 residue was more accessible to cellulases action. However, from Table 2, it is observed that a large part of the polysaccharides was removed during the *Organosolv* reaction. Thus, in the pretreated bagasse recovered after the Mo_2C/Al_2O_3–*Organosolv* treatment, a lower cellulose content was available in the pretreated bagasse to be converted by the enzymes, leading to a lower glucose concentration value (6.1 g L^{-1}).

Therefore, the treatments may have impacted the cellulose structure. Figure S2 depicts the thermogravimetric curves (TG) and their first derivative curves (DTG) of pretreated bagasse obtained under different treatments. The thermal degradation of hemicellulose and cellulose occurs at temperatures close to 330 °C for untreated residues [57]. Lignin and hemicellulose initiate degradation at lower temperatures than

817 cellulose. Lignin has a wide range of degradation, close to 237-510 °C. Cellulose,
818 however, degrades between 374-425 °C and hemicellulose between 288-382 °C, which
819 can be observed as a shoulder in the DTG of untreated bagasse. This shoulder is also a
820 result of lower molecular weight components such as extractives [57].

821 DTG curves revealed that the impact of the treatment on cellulose was higher for
822 samples treated with Mo_2C catalysts, since there is considerable variation in the
823 maximum temperature peak. The Mo_2C type catalysts presented a decrease in the
824 maximum temperature in the DTG, which may be related to a facilitated degradation of
825 cellulose due to structural modifications affecting its stability [58], when compared to
826 iPrOH treatment and in the presence of Raney-Ni catalyst. It should also be considered
827 that the exposure of the cellulose favored the enzymatic action and consequently, the
828 increase in the glucose yield of the pretreated samples, consistent with results presented
829 in Fig. 10.

830 Aiming at getting further insights regarding lignin distribution and cellulose
831 exposure in the pretreated bagasse samples, confocal microscopy analysis was
832 performed (Fig. 11). The images were treated with the software using the histogram
833 stretching mode to provide greater contrast between the structures. Images were
834 obtained in different spectral regions for lignin and cellulose observation; thus Fig. 11
835 shows the overlay of both images. The original microscopy images without histogram
836 stretching are provided in Fig. S3. It could be observed that the lignin (red color) and
837 cellulose (green color) structures are practically intact on the untreated bagasse,
838 showing intact cell walls. After treatment, fibrous and porous surfaces are observed,
839 except for the Ni+iPrOH residue because it had a more compact surface. Furthermore,
840 the unprocessed images (Fig. S3) reveal that the surface of the residues are covered by
841 the lignin structure (red), except for the Mo_2C/AC+iPrOH pretreated bagasse that

exposes the cellulose structure (green). In Fig. S3 (E) it is possible to see that this is the only sample in which cellulose is clearly exposed in its surface, correlating well with the improved enzymatic hydrolysis yields obtained for this residue. In particular, as show in Table 2, the treatment with Mo_2C/AC+iPrOH resulted in an increased removal of cellulose and hemicellulose, but the remaining polysaccharides became more accessible to the hydrolysis.

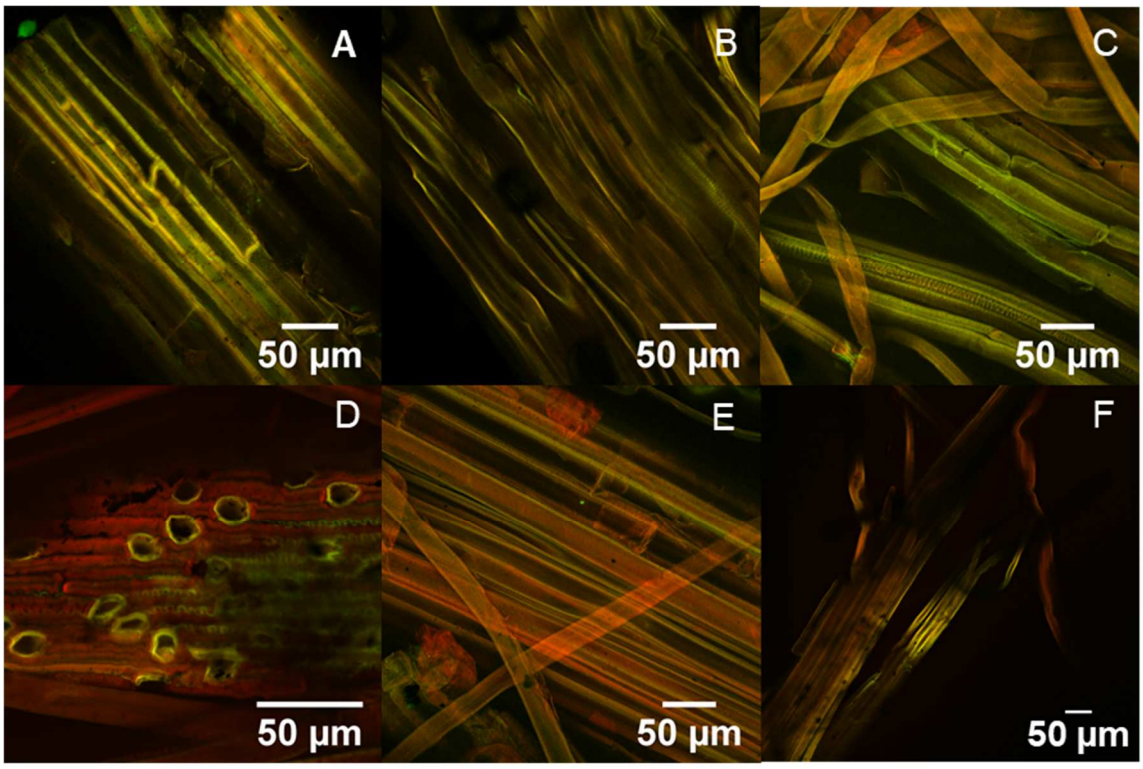

Figure 11. Confocal micrographs of the distribution of cellulose and lignin in pretreated bagasse samples processed with the software in histogram stretching mode. Red fluorescent signs identify the lignin structure and green signal identifies the structure of the cellulose. Residues: A) untreated bagasse, B) iPrOH, C) Ni+iPrOH, D) Mo_2C+iPrOH, E) Mo_2C/AC+iPrOH, F) Mo_2C/Al_2O_3+iPrOH.

Additionally, by correlating these observations with the data presented in Table S1, it is possible to conclude that the samples derived from conditions with high lignin

858 content presented an intense red color (Fig. 11, E and F). However, for conditions that
859 resulted in low lignin content in the bagasse residue (Fig. 11, C and D), the
860 predominance of red color in some areas could also be observed.

861 This observation could also be partially related to a possible condensation and/or
862 repolymerization of the previously depolymerized smaller fragments formed followed
863 by their deposition on the surface of the solid residue. This repolymerized lignin is
864 characterized by very strong C—C bonds that are highly recalcitrant in relation to the
865 C—O bonds characteristic of native lignin, making this material less susceptible to
866 enzymatic attack. In the reaction, the solvent extracts lignin from the lignocellulosic
867 matrix and breaks the α-O-4 ether bonds, resulting in the formation of unsaturated
868 phenolic intermediates. During Organosolv treatment, α-O-4 bonds in the lignin
869 structure are cleaved predominantly, and the β-O-4 linkages remains unreacted due to
870 the lower activation energy for cleavage of α-O-4 bonds [59]. The catalyst in turn is
871 responsible for the hydrogenation of the reactive unsaturated side chains of the lignin
872 intermediates that have been solubilized, leading to the formation of stable phenolic
873 monomers and avoiding undesirable reactions of repolymerization [19]. By correlating
874 the confocal images and the enzymatic hydrolysis results, it is suggested that the
875 Mo_2C/AC could be a better hydrogenation catalyst thus avoiding the lignin
876 repolymerization on the surface of the pretreated bagasse and, consequently favoring the
877 enzymatic hydrolysis. Therefore, this indicates that not only the content, but also the
878 lignin distribution affects the cell wall recalcitrance to the enzymatic depolymerization.

879 A similar result was reported by Santo *et al*. [60]. These authors evaluated the
880 compositional and structural changes on sugarcane bagasse caused by hydrothermal
881 and/or *Organosolv* (ethanol) treatments. They found that the treatments resulted in

lignin degradation, rearrangement and inhomogeneous deposition of significant amounts of lignin on the surface of the treated residue.

Despite of the apparent low delignification, the hydrolysis of the bagasse treated by Mo_2C/AC+iPrOH achieved 67 % glucose yield (13.7 g L^{-1} glucose). This is a promising result, showing that the production of bio-oil from bagasse could be associated with production of cellulosic ethanol, giving a proper use to distinct biomass fractions.

4. Conclusion

The *Organosolv* treatment of sugarcane bagasse caused a partial extraction of hemicellulose from the pretreated bagasse through the solvolysis performed by the isopropanol/water mixture. The extent of hemicellulose extraction from the pretreated bagasse varied in the following order: without catalyst ≈ Raney-Ni << bulk Mo_2C ≈ Mo_2C/Al_2O_3 < Mo_2C/AC. High recovery of cellulose in the solid residue was achieved in the absence of catalyst and with Raney-Ni but the recovered fraction of cellulose decreased on Mo_2C-based catalysts. After solvolytic extraction, hemicellulose was depolymerized and product distribution obtained depended on the type of active phase. Raney-Ni catalyst promoted the formation of diols (1,2-butanediol, 1,4-butanediol) and triols (glycerol, 1,2,4-butanetriol), while xylose, furfural, and furan were mainly produced by Mo_2C based-catalysts.

The catalyst also influenced the product distribution obtained from lignin depolymerization, which depended on the active phase. The *Organosolv* treatment without catalyst and in the presence of bulk Mo_2C and Mo_2C/AC catalysts produced significant amount of 2,3-dihydrobenzofuran, whereas this

907 compound was detected in trace amounts in the bio-oil obtained from Raney-Ni
908 and Mo_2C/Al_2O_3. This product stem from the depolymerization of
909 phenylcoumaran structures characteristic of lignin from grasses such as sugarcane
910 bagasse and it is not formed on the catalytic fractionation of hardwoods and
911 softwoods.

912 Mo_2C-based catalysts favored the formation of substituted
913 methoxyphenols but product distribution depended on the active phase.
914 Cyclohexanepropanoic acid, 3,4-dihydroxycyclohexanepropanoic acid and
915 benzylmalonic acid were only formed on Raney-Ni catalyst, whereas substituted
916 methoxyphenols such as 3-hydroxy-4-methoxybenzaldehyde and 2,6-dimethoxy-
917 4-(2-propenyl)-phenol were formed over Mo_2C/Al_2O_3 catalyst. These results
918 were likely due to the capacity of the active phase to promote the cleavage of
919 specific C-O and C-C bonds, originating different substituted methoxyphenols.
920 For Raney-Ni, benzylmalonic acid is obtained by the cleavage of β-O-4 bonds of
921 the ferulate unit, while 3,5-dimethoxy-4-hydroxycinnamaldehyde
922 (sinapaldehyde) is produced by breaking β-O-4 and α-O-5 bonds of a guaiacyl
923 unit. The Mo_2C/AC and Mo_2C/Al_2O_3 catalysts exhibited the highest yield to
924 substituted methoxyphenols (~ 24%), which is similar to the values reported in
925 the literature for bio-oil from catalytic fractionation of sugarcane bagasse but at
926 less severe reaction conditions.

927 The enzymatic hydrolysis of the solid residue obtained from the
928 *Organosolv* treatment of sugarcane bagasse without catalyst and with Raney-Ni
929 resulted in very low glucose concentration and yield. The fractionation with Mo_2C/AC
930 generated a pretreated bagasse that was readily hydrolyzed by cellulases, producing
931 glucose yield and concentration of 67 % and 13.7 g L^{-1}, respectively. TG experiments

revealed that the cellulose structure was differently affected by the treatment depending on the catalyst. DTG curves showed lower stability of cellulose treated with Mo_2C catalysts, which is likely due to structural modifications that occurred during fractionation. Confocal microscopy analysis confirmed that cellulose structure is more exposed after treatment with Mo_2C/AC catalyst, which favored the enzymatic action and consequently, the highest glucose yield obtained for this residue.

Therefore, Mo_2C/AC and Mo_2C/Al_2O_3 are promising catalysts for the fractionation of sugarcane bagasse that produced a bio-oil with higher yield to substituted methoxyphenols and a solid residue more easily hydrolyzed by cellulases, producing higher yield to glucose than Raney-Ni catalyst.

Acknowledgements

The authors thank CAPES (Finance code001), CNPq (303667/2018-4; 305046/2015-2), FAPERJ (E-26/202.783/2017) and Office of Naval Research (N62909-18-1-2085) for the scholarship and the financial support.

REFERENCES

[1] L.R. Lynd, X. Liang, M.J. Biddy, A. Allee, H. Cai, T. Foust, M.E. Himmel, M.S. Laser, M. Wang, C.E. Wyman, Cellulosic ethanol: status and innovation, Curr. Opin. Biotechnol. 45 (2017) 202–211. https://doi.org/10.1016/j.copbio.2017.03.008.

[2] A.K. Chandel, V.K. Garlapati, A.K. Singh, F.A.F. Antunes, S.S. da Silva, The path forward for lignocellulose biorefineries: Bottlenecks, solutions, and

perspective on commercialization, Bioresour. Technol. 264 (2018) 370–381. https://doi.org/10.1016/j.biortech.2018.06.004.

[3] T. Renders, S. Van den Bosch, S.-F. Koelewijn, W. Schutyser, B.F. Sels, Lignin-first biomass fractionation: the advent of active stabilisation strategies, Energy Environ. Sci. 10 (2017) 1551–1557. https://doi.org/10.1039/C7EE01298E.

[4] R. Rinaldi, R. Jastrzebski, M.T. Clough, J. Ralph, M. Kennema, P.C.A. Bruijnincx, B.M. Weckhuysen, Paving the Way for Lignin Valorisation: Recent Advances in Bioengineering, Biorefining and Catalysis, Angew. Chemie Int. Ed. 55 (2016) 8164–8215. https://doi.org/10.1002/anie.201510351.

[5] J. Zakzeski, P. C. A. Bruijnincx, A. L. Jongerius, B. M. Weckhuysen, The catalytic valorization of lignin for the production of renewable chemicals, Chem. Rev. 110 (2010) 3552-3599. https://doi.org/10.1021/cr900354u.

[6] W. Schutyser, S. Van Den Bosch, T. Renders, T. De Boe, S.F. Koelewijn, A. Dewaele, T. Ennaert, O. Verkinderen, B. Goderis, C.M. Courtin, B.F. Sels, Influence of bio-based solvents on the catalytic reductive fractionation of birch wood, Green Chem. 17 (2015) 5035–5045. https://doi.org/10.1039/c5gc01442e.

[7] L. Shuai, J. Luterbacher, Organic Solvent Effects in Biomass Conversion Reactions, ChemSusChem. 9 (2016) 133–155. https://doi.org/10.1002/cssc.201501148.

[8] Z. Chen, J. Long, Organosolv liquefaction of sugarcane bagasse catalyzed by acidic ionic liquids, Bioresour. Technol. 214 (2016) 16–23. https://doi.org/10.1016/j.biortech.2016.04.089.

[9] S.X. Li, M. F. Li, P. Yu, Y. M. Fan, J. N. Shou, R. C. Sun, Valorization of bamboo by γ-valerolactone/acid/water to produce digestible cellulose, degraded

sugars and lignin, Bioresour. Technol. 230 (2017) 90-96. https://doi.org/10.1016/j.biortech.2017.01.041.

[10] P. Ferrini, R. Rinaldi, Catalytic biorefining of plant biomass to non-pyrolytic lignin bio-oil and carbohydrates through hydrogen transfer reactions, Angew. Chemie Int. Ed. 53 (2014) 8634–8639. https://doi.org/10.1002/anie.201403747.

[11] Y. Wang, X. Pan, Y. Ye, S. Li, D. Wang, Y.Q. Liu, Process optimization of biomass liquefaction in isopropanol/water with Raney nickel and sodium hydroxide as combined catalysts, Biomass Bioenerg. 122 (2019) 305–312. https://doi.org/10.1016/j.biombioe.2019.01.020.

[12] L. Mesa, N. Lopez, C. Cara, E. Castro, E. Gonzalez, S.I. Mussatto, Techno-economic evaluation of strategies based on two steps organosolv pretreatment and enzymatic hydrolysis of sugarcane bagasse for ethanol production, Renew. Energy 86 (2016) 270–279.

[13] H. Zhang, S. Wu, Efficient sugar release by acetic acid ethanol-based organosolv pretreatment and enzymatic saccharification, J. Agric. Food Chem. 62 (2014) 11681–11687. https://doi.org/10.1021/jf503386b.

[14] M. Grilc, B. Likozar, J. Levec, Hydrotreatment of solvolytically liquefied lignocellulosic biomass over NiMo/Al_2O_3 catalyst: Reaction mechanism, hydrodeoxygenation kinetics and mass transfer model based on FTIR, Biomass Bioenergy 63 (2014) 300-312.

[15] M. Grilc, B. Likozar, J. Levec, Hydrodeoxygenation and hydrocracking of solvolysed lignocellulosic biomass by oxide, reduced and sulphide form of NiMo, Ni, Mo and Pd catalysts, App. Catal. B 150 (2014) 275-287.

[16] M. Grilc, B. Likozar, J. Levec, Simultaneous Liquefaction and Hydrodeoxygenation of Lignocellulosic Biomass over NiMo/Al_2O_3, Pd/Al_2O_3,

and Zeolite Y Catalysts in Hydrogen Donor Solvents, ChemCatChem. 8 (2016) 180–191. https://doi.org/10.1002/cctc.201500840.

[17] M. V. Galkin, S. Sawadjoon, V. Rohde, M. Dawange, J.S.M. Samec, Mild heterogeneous palladium-catalyzed cleavage of β-O-4'-ether linkages of lignin model compounds and native lignin in air, ChemCatChem. 6 (2014) 179–184. https://doi.org/10.1002/cctc.201300540.

[18] L. Shuai, Y.M. Questell-Santiago, J.S. Luterbacher, A mild biomass pretreatment using γ-valerolactone for concentrated sugar production, Green Chem. 18 (2016) 937–943. https://doi.org/10.1039/C5GC02489G.

[19] S. Van den Bosch, T. Renders, S. Kennis, S.-F. Koelewijn, G. Van den Bossche, T. Vangeel, A. Deneyer, D. Depuydt, C.M. Courtin, J. Thevelein, W. Schutyser, B.F. Sels, Integrating lignin valorization and bio-ethanol production: on the role of Ni-Al_2O_3 catalyst pellets during lignin-first fractionation, Green Chem. 19 (2017) 3313-3326. https://doi.org/10.1039/C7GC01324H.

[20] Q. Song, F. Wang, J. Cai, Y. Wang, J. Zhang, W. Yu, J. Xu, Lignin depolymerization (LDP) in alcohol over nickel-based catalysts via a fragmentation-hydrogenolysis process, Energy Environ. Sci. 6 (2013) 994–1007. https://doi.org/10.1039/c2ee23741e.

[21] N. Yan, C. Zhao, P.J. Dyson, C. Wang, L.T. Liu, Y. Kou, Selective degradation of wood lignin over noble-metal catalysts in a two-step process, ChemSusChem. 1 (2008) 626–629. https://doi.org/10.1002/cssc.200800080.

[22] C.R. Lee, J.S. Yoon, Y.W. Suh, J.W. Choi, J.M. Ha, D.J. Suh, Y.K. Park, Catalytic roles of metals and supports on hydrodeoxygenation of lignin monomer guaiacol, Catal. Commun. 17 (2012) 54–58. https://doi.org/10.1016/j.catcom.2011.10.011.

1031 [23] X. Wang, R. Rinaldi, Exploiting H-transfer reactions with RANEY® Ni for
1032 upgrade of phenolic and aromatic biorefinery feeds under unusual, low-severity
1033 conditions, Energy Environ. Sci. 5 (2012) 8244–8260.
1034 https://doi.org/10.1039/c2ee21855k.
1035 [24] E.F. Mai, M.A. Machado, T.E. Davies, J.A. Lopez-Sanchez, V. Teixeira Da
1036 Silva, Molybdenum carbide nanoparticles within carbon nanotubes as superior
1037 catalysts for γ-valerolactone production via levulinic acid hydrogenation, Green
1038 Chem. 16 (2014) 4092–4097. https://doi.org/10.1039/c4gc00920g.
1039 [25] J. Pang, J. Sun, M. Zheng, H. Li, Y. Wang, T. Zhang, Transition metal carbide
1040 catalysts for biomass conversion: A review, Appl. Catal. B Environ. 254 (2019)
1041 510–522. https://doi.org/10.1016/j.apcatb.2019.05.034.
1042 [26] M.A. Machado, S. He, T.E. Davies, K. Seshan, V. Teixeira, Renewable fuel
1043 production from hydropyrolysis of residual biomass using molybdenum
1044 carbide-based catalysts : An analytical Py-GC / MS investigation, Catal. Today.
1045 302 (2018) 161–168. https://doi.org/10.1016/j.cattod.2017.06.024.
1046 [27] X. Yang, M. Feng, J.S. Choi, H.M. Meyer, B. Yang, Depolymerization of corn
1047 stover lignin with bulk molybdenum carbide catalysts, Fuel. 244 (2019) 528–
1048 535. https://doi.org/10.1016/j.fuel.2019.02.023.
1049 [28] M. Grilc, G. Veryasov, B. Likozar, A. Jesih, J. Levec, Hydrodeoxygenation of
1050 solvolysed lignocellulosic biomass by unsupported MoS_2, MoO_2, Mo_2C and
1051 WS_2 catalysts, Appl. Catal. B Environ. 163 (2015) 467–477.
1052 https://doi.org/10.1016/j.apcatb.2014.08.032.
1053 [29] C. Li, M. Zheng, A. Wang, T. Zhang, One-pot catalytic hydrocracking of raw
1054 woody biomass into chemicals over supported carbide catalysts: simultaneous

conversion of cellulose, hemicellulose and lignin, Energy Environ. Sci. 5 (2012) 6383–6390. https://doi.org/10.1039/C1EE02684D.

[30] Z. Sun, B. Fridrich, A. De Santi, S. Elangovan, K. Barta, Bright Side of Lignin Depolymerization: Toward New Platform Chemicals, Chem. Rev. 118 (2018) 614–678. https://doi.org/10.1021/acs.chemrev.7b00588.

[31] H. Luo, I.M. Klein, Y. Jiang, H. Zhu, B. Liu, H.I. Kenttämaa, M.M. Abu-Omar, Total Utilization of Miscanthus Biomass, Lignin and Carbohydrates, Using Earth Abundant Nickel Catalyst, ACS Sustain. Chem. Eng. 4 (2016) 2316–2322. https://doi.org/10.1021/acssuschemeng.5b01776.

[32] A. Sluiter, B. Hames, R. Ruiz, C. Scarlata, J. Sluiter, D. Templeton, D. Crocker, 2012. Determination of structural carbohydrates and lignin in biomass: Laboratory Analytical Procedure (LAP), NREL/TP-510-42618. National Renewable Energy Laboratory (NREL), Golden, Colorado, USA.

[33] B. Adney, J. Baker, 2008, Measurement of cellulose activities laboratory analytical procedure. Technical Report NREL/TP-510-42628, National Renewable Energy Laboratory.

[34] J. Han, J. Duan, P. Chen, H. Lou, H. Hong, Nanostructured molybdenum carbides supported on carbon nanotubes as efficient catalysts for one-step hydrodeoxygenation and isomerization of vegetable oils, Green Chem.13 (2011) 2561–2568. https://doi.org/10.1039/c1gc15421d.

[35] A.S. Rocha, L.A. Souza, R.R. Oliveira, A.B. Rocha, V. Teixeira, Hydrodeoxygenation of acrylic acid using Mo_2C/Al_2O_3, App. Catal. A Gen. 531 (2017) 69–78. https://doi.org/10.1016/j.apcata.2016.12.009.

[36] L.P. Novo, L.V.A Gurgel, K. Marabezi, A.A.S. Curvelo, Delignification of sugarcane bagasse using glycerol–water mixtures to produce pulps for

saccharification. Biores. Technol. 102 (2011) 10040-10046. https://10.1016/j.biortech.2011.08.050.

[37] L.C.A. Barbosa, C.R. Maltha, V.L. Silva, J.L. Colodette, Determinação da relação siringila/guaiacila da lignina em madeiras de eucalipto por pirólise acoplada à cromatografia gasosa e espectrometria de massas (PI-CG/EM), Quim. Nova. 31 (2008) 2035–2041. https://doi.org/10.1590/S0100-40422008000800023.

[38] J.S. Lupoi, S. Singh, R. Parthasarathi, B.A. Simmons, R.J. Henry, Recent innovations in analytical methods for the qualitative and quantitative assessment of lignin, Renew. Sustain. Energy Rev. 49 (2015) 871–906. https://doi.org/10.1016/j.rser.2015.04.091.

[39] S. Van den Bosch, W. Schutyser, R. Vanholme, T. Driessen, S.-F. Koelewijn, T. Renders, B. De Meester, W.J.J. Huijgen, W. Dehaen, C.M. Courtin, B. Lagrain, W. Boerjan, B.F. Sels, Reductive lignocellulose fractionation into soluble lignin-derived phenolic monomers and dimers and processable carbohydrate pulps, Energy Environ. Sci. 8 (2015) 1748–1763. https://doi.org/10.1039/C5EE00204D.

[40] F. Melligan, M.H.B. Hayes, W. Kwapinski, J.J. Leahy, Hydro-Pyrolysis of Biomass and Online Catalytic Vapor Upgrading with Ni-ZSM -5 and Ni-MCM-41, 26 (2012) 6080-6090. https://doi.org/10.1021/ef301244h.

[41] X. Hu, S. Jiang, S. Kadarwati, D. Dong, C.Z. Li, Effects of water and alcohols on the polymerization of furan during its acid-catalyzed conversion into benzofuran, RSC Adv. 6 (2016) 40489–40501. https://doi.org/10.1039/c6ra04745a.

[42] M.M. Abu-Omar, K. Barta, G.T. Beckham, J.S. Luterbacher, J. Ralph, R. Rinaldi, Y. Román-Leshkov, J.S.M. Samec, B.F. Sels, F. Wang, Guidelines for performing lignin-first biorefining, Energy Environ. Sci. 14 (2021) 262–292. https://doi.org/10.1039/d0ee02870c.

[43] E. Ilya, L. Kulikova, E. V. Van der Eycken, L. Voskressensky, Recent Advances in Phthalan and Coumaran Chemistry, ChemistryOpen. 7 (2018) 914–929. https://doi.org/10.1002/open.201800184.

[44] J.A.S. Barros, M.C. Krause, E. Lazzari, T.R. Bjerk, A.L. do Amaral, E.B. Caramão, L.C. Krause, Chromatographic characterization of bio-oils from fast pyrolysis of sugar cane residues (straw and bagasse) from four genotypes of the Saccharum Complex, Microchem. J. 137 (2018) 30–36. https://doi.org/10.1016/j.microc.2017.09.015.

[45] K. Srinivas, F. de Carvalho Oliveira, P.J. Teller, A.R. Gonçalves, G.L. Helms, B.K. Ahring, Oxidative degradation of biorefinery lignin obtained after pretreatment of forest residues of Douglas Fir, Bioresour. Technol. 221 (2016) 394–404. https://doi.org/10.1016/j.biortech.2016.09.040.

[46] A.L. Flourat, A. Haudrechy, F. Allais, J.-H. Renault, (S)-γ-Hydroxymethyl-α,β-butenolide, a valuable chiral synthon: syntheses, reactivity, and applications, Org. Process Res. Dev. 24 (2020) 615–636. https://doi.org/10.1021/acs.oprd.9b00468.

[47] G.J. de M. Rocha, V.M. Nascimento, A.R. Gonçalves, V.F.N. Silva, C. Martín, Influence of mixed sugarcane bagasse samples evaluated by elemental and physical-chemical composition, Ind. Crops Prod. 64 (2015) 52–58. https://doi.org/10.1016/j.indcrop.2014.11.003.

1128 [48] C.I. Santos, C.C. Silva, S.I. Mussatto, P. Osseweijer, L.A.M. van der Wielen,
1129 J.A. Posada, Integrated 1st and 2nd generation sugarcane bio-refinery for jet
1130 fuel production in Brazil: Techno-economic and greenhouse gas emissions
1131 assessment, Renew. Energy. 129 (2018) 733–747.
1132 https://doi.org/10.1016/j.renene.2017.05.011.
1133 [49] S. Chen, R. Wojcieszak, F. Dumeignil, E. Marceau, S. Royer, How Catalysts
1134 and Experimental Conditions Determine the Selective Hydroconversion of
1135 Furfural and 5-Hydroxymethylfurfural, Chem. Rev. 118 (2018) 11023–11117.
1136 https://doi.org/10.1021/acs.chemrev.8b00134.
1137 [50] Y. Nakagawa, T. Kasumi, J. Ogihara, M. Tamura, T. Arai, K. Tomishige,
1138 Erythritol: Another C4 Platform Chemical in Biomass Refinery, ACS Omega. 5
1139 (2020) 2520-2530.
1140 [51] W. Lv, Y. Liao, Y. Zhu, J. Liu, C. Zhu, C. Wang, Y. Xu, Q. Zhang, G. Chen,
1141 L. Ma, The effect of Ru/C and $MgCl_2$ on the cleavage of inter- and intra-
1142 molecular linkages during cornstalk hydrolysis residue valorization, Cellulose
1143 27 (2020) 799-823. https://doi.org/10.1007/s10570-019-02799-x.
1144 [52] D.J. Hayes, An examination of biorefining processes, catalysts and challenges,
1145 Catal. Today. 145 (2009) 138–151.
1146 https://doi.org/10.1016/j.cattod.2008.04.017.
1147 [53] S. Van Den Bosch, W. Schutyser, S.F. Koelewijn, T. Renders, C.M. Courtin,
1148 B.F. Sels, Tuning the lignin oil OH-content with Ru and Pd catalysts during
1149 lignin hydrogenolysis on birch wood, Chem. Commun. 51 (2015) 13158–
1150 13161. https://doi.org/10.1039/c5cc04025f.
1151 [54] L. M.C. L. K. Curran, L. T. M. Pham, K.L. Sale, B. A. Simmons. Review of
1152 advances in the development of laccases for the valorization of lignin to enable

1153 the production of lignocellulosic biofuels and bioproducts, Biotechnol. Adv.
1154 (2021) 107809. https://doi.org/10.1016/j.biotechadv.2021.107809
1155 [55] A. Susmozas, R. Mantín-Sampedro, D. Ibarra, M. E. Eugenio, R. Iglesias, P.
1156 Manzanares, A. D. Moreno. Processes 8 (2020) 1310.
1157 https://doi.org/10.3390/pr8101310
1158 [56] M.V. Galkin, A.T. Smit, E. Subbotina, K.A. Artemenko, J. Bergquist, W.J.J.
1159 Huijgen, J.S.M. Samec, Hydrogen-free catalytic fractionation of woody
1160 biomass, ChemSusChem. 9 (2016) 3280-3287.
1161 http://dx.doi.org/10.1002/cssc.201600648.
1162 [57] O.M. Perrone, F.M. Colombari, J.S. Rossi, M.M.S. Moretti, S.E. Bordignon, C.
1163 da C.C. Nunes, E. Gomes, M. Boscolo, R. Da-Silva, Ozonolysis combined with
1164 ultrasound as a pretreatment of sugarcane bagasse: Effect on the enzymatic
1165 saccharification and the physical and chemical characteristics of the substrate,
1166 Bioresour. Technol. 218 (2016) 69–76.
1167 https://doi.org/10.1016/j.biortech.2016.06.072.
1168 [58] M. Brebu, C. Vasile, Thermal degradation of lignin – A review. Cell. Chem.
1169 Technol. 44 (2010) 353-363.
1170 [59] E. Jasiukaitytè-Grojzdek, M. Huš, M. Grilc, B. Likozar, Acid-catalysed α-O-4
1171 aryl-ether bond cleavage in methanol/ (aqueous) ethanol: understanding
1172 depolymerisation of a lignin model compound during organosolv pretreatment,
1173 Nature. 10 (2020) 11037. https://doi.org/10.1038/s41598-020-67787-92
1174 [60] M. Espirito Santo, C.A. Rezende, O.D. Bernardinelli, N. Pereira, A.A.S.
1175 Curvelo, E.R. deAzevedo, F.E.G. Guimarães, I. Polikarpov, Structural and
1176 compositional changes in sugarcane bagasse subjected to hydrothermal and

1177 organosolv pretreatments and their impacts on enzymatic hydrolysis, Ind. Crops
1178 Prod. 113 (2018) 64–74. https://doi.org/10.1016/j.indcrop.2018.01.014.

Graphical Abstract